



**Calhoun: The NPS Institutional Archive**  
**DSpace Repository**

---

Theses and Dissertations

1. Thesis and Dissertation Collection, all items

---

1949

# Investigation of a sandwich type circular plate under transverse loading.

Gates, Clark Harrison

California Institute of Technology

---

<http://hdl.handle.net/10945/6469>

---

*Downloaded from NPS Archive: Calhoun*



Calhoun is the Naval Postgraduate School's public access digital repository for research materials and institutional publications created by the NPS community. Calhoun is named for Professor of Mathematics Guy K. Calhoun, NPS's first appointed -- and published -- scholarly author.

**Dudley Knox Library / Naval Postgraduate School**  
**411 Dyer Road / 1 University Circle**  
**Monterey, California USA 93943**

<http://www.nps.edu/library>

NPS ARCHIVE  
1949  
GATES, C.

Thesis  
G25

Thesis  
G25

DUDLEY KNOX LIBRARY  
NAVAL POSTGRADUATE SCHOOL  
MONTEREY CA 93943-5101

Library  
U. S. Naval Postgraduate School  
Annapolis, Md.







INVESTIGATION OF A SUSPECTED FIVE FIFTEEN FIFTY FIFTY

THIRTEEN FIFTY

THIRTEEN FIFTY

THIRTEEN FIFTY

THIRTEEN FIFTY

IN THIRTEEN FIFTY

THIRTEEN FIFTY

THIRTEEN FIFTY

THIRTEEN FIFTY



INVESTIGATION OF A SANDWICH TYPE CIRCULAR PLATE UNDER  
TRANSVERSE LOADING

A Thesis  
Submitted to the Graduate Faculty  
of the  
University of Minnesota

by  
*Clark H. Gates*  
CLARK H. GATES

In Partial Fulfillment of the Requirements  
for the  
Degree of Master of Science in Aeronautical Engineering

August 1949



1949

GATES, C

THESE ARE THE ONLY TWO COPIES OF THE ORIGINAL

RECORDS AVAILABLE

~~TOP SECRET~~

SECRET

ALL INFORMATION CONTAINED HEREIN IS UNCLASSIFIED

DATE 11

EXCEPT WHERE SHOWN OTHERWISE

TOP SECRET

ALL INFORMATION CONTAINED HEREIN IS UNCLASSIFIED

DATE 11

EXCEPT WHERE SHOWN OTHERWISE

SECRET

## PREFACE

The influence of shear deformation on the behavior of a sandwich-type aircraft structural panel under load has been treated at length analytically and experimentally. However, as far as is known, experimentation is not complete in attempting to actually measure the shearing stresses causing this deformation.

A problem of interest, as pointed out by engineers of Chance Vought Aircraft, would be a study of the distribution of these shearing stresses in the core of a sandwich plate, such as Metalite. More specifically, the project the writer had in mind at the beginning of this work was to determine the distribution of transverse shear stresses along the boundaries of a simply supported rectangular Metalite panel subjected to a uniformly distributed normal load.

First, however, it was necessary to find an adequate testing method for measuring these stresses. Developing upon a unique idea suggested by Prof. J. A. Wise, University of Minnesota, such a method for experimentally determining the actual shearing stresses occurring in the core was attempted.

Time consuming difficulties arising in the perfecting of this testing procedure prevented the writer from applying it to his originally chosen problem mentioned above. However, the method was tested on a circular panel and partial success was realized, the results obtained and the testing method as developed being presented herein.



The writer wishes to acknowledge the material aid and technical assistance given him by E. A. Fitman, Boone T. Guyton, as well as others, of Chance Vought aircraft, Dallas, Texas. Appreciation is also extended both to Prof. J. A. Wise, thesis adviser, for his suggestions and guidance in the preparation of this paper, and to E. B. Johnson for his assistance and the use of his experimental testing equipment.





## TABLE OF CONTENTS

	Page
PREFACE . . . . .	11
SUMMARY . . . . .	v
INTRODUCTION . . . . .	1
TESTING EQUIPMENT AND PROCEDURE . . . . .	6
RESULTS AND DISCUSSION . . . . .	10
CONCLUSIONS . . . . .	16
APPENDIX A: Theory of Reflection and Face Stresses . .	17
APPENDIX B: Problems Concerning the Use of the Single Wire Strain Gage . . . . .	32
REFERENCES AND BIBLIOGRAPHY . . . . .	33
TABLES . . . . .	36
FIGURES . . . . .	38



TABLE 20

1927

11	.....	.....
12	.....	.....
13	.....	.....
14	.....	.....
15	.....	.....
16	.....	.....
17	.....	.....
18	.....	.....
19	.....	.....
20	.....	.....
21	.....	.....
22	.....	.....
23	.....	.....
24	.....	.....
25	.....	.....

## SUMMARY

This thesis presents the results of an investigation where an attempt was made to indirectly measure transverse shear stresses in the balsa core of a Metalite (sandwich-type) plate by use of a single wire electrical strain gage passed through the thickness of the core at  $45^\circ$ . Conditions were limited to a simply supported circular panel subjected to a uniformly distributed normal load.

Although the test method for shear stress developed herein was only partially successful, the results indicate that it may be a feasible one but further investigation is necessary to substantiate the results obtained here and to improve upon the technique used.

Consideration was also given to the deflection curve of the panel under load and to the resulting planar stresses in the faces of sandwich plate. Due to friction conditions existing between the support and the plate, the desired simple support was not fully realized. However, test deflections show fair agreement with analytical theory for the lower loading values.



## INTRODUCTION

The problem under consideration in this thesis consists mainly of the development of an experimental testing method for measuring the transverse shearing stresses occurring in the balsa core at the circumferential boundary of a Metalite sandwich-type circular plate. The panel was simply supported and was subjected to a uniform normal load.

A second and subsequent issue is the measurement of these boundary stresses, by this testing method, and their comparison with analytical predictions. Also of minor concern, but still a matter of interest, are the deflection curves of the Metalite panel during the test and the stresses occurring in the aluminum faces.

Considerable analytical study, (ref. 1, 2 & 3), has been made of shear deformation, the result of shear stress in the core of sandwich material, and some experimental work has been accomplished (ref. 4 and 5). However, the distribution of shearing stresses in the core has not been completely resolved. Hence this experimental approach to the problem seemed warranted.

Once the procedure for measuring the desired stresses, as explained below under Equipment and Procedure, had been established, repeated normal loading tests in 1/4 psi. increments were made from 0 to 1-1/4 psi. on a 30 inch



# DISCUSSION

The present study contributes to the knowledge of the biology of the freshwater fish, *Carassius auratus*, by providing information on its reproductive behavior. The results of the present study are in agreement with those of other workers who have reported that the spawning season of *C. auratus* is from March to May. The present study also confirms the findings of other workers that the spawning season of *C. auratus* is from March to May. The present study also confirms the findings of other workers that the spawning season of *C. auratus* is from March to May.

The present study also confirms the findings of other workers that the spawning season of *C. auratus* is from March to May. The present study also confirms the findings of other workers that the spawning season of *C. auratus* is from March to May. The present study also confirms the findings of other workers that the spawning season of *C. auratus* is from March to May. The present study also confirms the findings of other workers that the spawning season of *C. auratus* is from March to May. The present study also confirms the findings of other workers that the spawning season of *C. auratus* is from March to May.

The present study also confirms the findings of other workers that the spawning season of *C. auratus* is from March to May. The present study also confirms the findings of other workers that the spawning season of *C. auratus* is from March to May. The present study also confirms the findings of other workers that the spawning season of *C. auratus* is from March to May. The present study also confirms the findings of other workers that the spawning season of *C. auratus* is from March to May. The present study also confirms the findings of other workers that the spawning season of *C. auratus* is from March to May.

The present study also confirms the findings of other workers that the spawning season of *C. auratus* is from March to May. The present study also confirms the findings of other workers that the spawning season of *C. auratus* is from March to May. The present study also confirms the findings of other workers that the spawning season of *C. auratus* is from March to May. The present study also confirms the findings of other workers that the spawning season of *C. auratus* is from March to May. The present study also confirms the findings of other workers that the spawning season of *C. auratus* is from March to May.

diameter Metalite circular panel simply supported. Extreme care in minute adjustments were not at all times exercised where concerned with the minor issues, the effort being placed on an attempt to prove the method of test rather than obtain statistical results.

The sandwich panel used in the investigation was Metalite, produced by Chance Vought Aircraft of Dallas, Texas. Typical of most sandwich plates it has the two thin high-strength outer faces (aluminum alloy in this case) bonded to, and separated by, a relatively thick, low-density, low-stiffness core (and grain balsa). The following assumptions are made for the sandwich plate considered:

(1) Face parallel stresses in the core may be neglected so that all planar stresses are carried by the faces.

(2) The faces are very thin in comparison with the core.

(3) The neutral axis lies on the middle surface of the core.

(4) Shear stresses and shear deformation in planes perpendicular to the panel may be neglected in the facings because of their relatively high shear moduli. (Later tests, after reliability of this method has been perfected, may show that the faces may carry part of the transverse shear).

(5) Transverse shear forces are carried only by the core (this, too, may be disproved later) and these shear



Elementary behavior analysis (Bates, 1954) suggested that  
there is a close relationship between the two sides of the brain  
and the body. The left side of the brain is responsible for  
the control of the body's movements, while the right side is  
responsible for the control of the body's emotions.

The analysis of the body's movements in the laboratory was  
conducted by Bates (1954) and his colleagues. They found that  
the body's movements are controlled by the left side of the  
brain. The right side of the brain is responsible for the  
control of the body's emotions. The following are the results  
of the analysis of the body's movements in the laboratory:

(1) The body's movements are controlled by the left side of  
the brain. The right side of the brain is responsible for the  
control of the body's emotions.

(2) The body's movements are controlled by the left side of  
the brain. The right side of the brain is responsible for the  
control of the body's emotions.

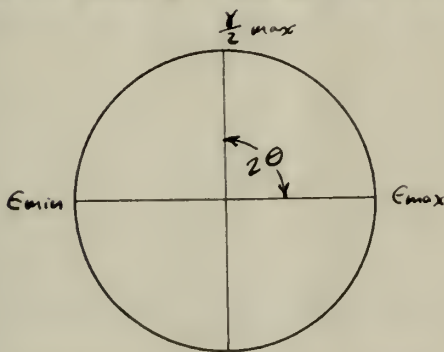
(3) The body's movements are controlled by the left side of  
the brain. The right side of the brain is responsible for the  
control of the body's emotions.

(4) The body's movements are controlled by the left side of  
the brain. The right side of the brain is responsible for the  
control of the body's emotions. The following are the results  
of the analysis of the body's movements in the laboratory:  
The body's movements are controlled by the left side of the  
brain. The right side of the brain is responsible for the  
control of the body's emotions. The following are the results  
of the analysis of the body's movements in the laboratory:

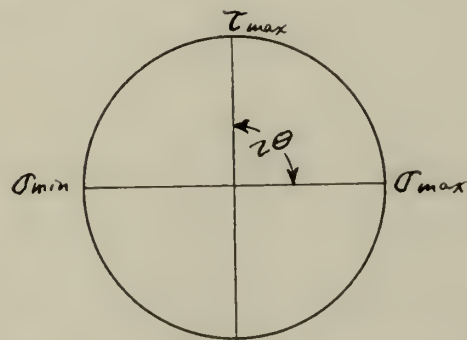
forces are distributed uniformly across the thickness of the core.

Considering a point on the neutral axis of the cross section of the sandwich material and applying the conditions prevailing there to a Mohr's circle of stress, it is seen that the shearing stress present is equal numerically to the two principal stresses and that these principal stresses are at a  $45^\circ$  angle to the plane of the plate. If the strain of this principal stress can be measured as it occurs in the core, then its stress can be determined and will be equal to the shearing stress at the neutral axis. Further, from assumption (5), this shearing stress will be constant across the cross section of the plate at that point.

The Mohr's circles of strain and stress mentioned above can be shown as follows:



Mohr's Circle of Strain



Mohr's Circle of Stress

From Theory of Elasticity:

$$\sigma_{\max} = \frac{E}{1-\mu^2} (\epsilon_{\max} + \mu \epsilon_{\min}) \quad \text{Eq. 1}$$

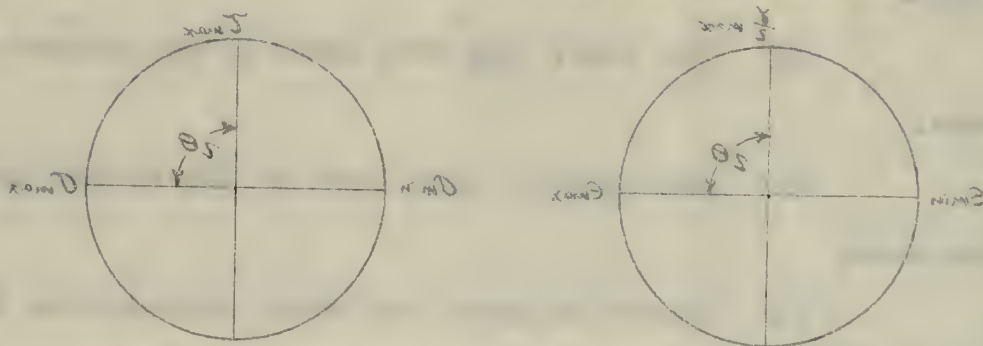
In the strain circle above,

$$\epsilon_{\max} = -\epsilon_{\min}$$

forces are distributed uniformly across the thickness of the plate.

Consider a point on the central axis of the plate section at the distance  $x$  from the left end. The distance from the right end is  $l-x$ . The forces acting on the element of length  $dx$  are the normal stresses  $\sigma_x$  and  $\sigma_{x+dx}$  acting on the faces of area  $A$ , and the weight  $W = \rho A dx$  acting downwards. The equilibrium of the element gives the differential equation  $\frac{d\sigma}{dx} = -\rho$ . Integrating this equation, we get  $\sigma = -\rho x + C_1$ . The boundary condition at the right end ( $x=l$ ) is that the stress is zero, i.e.,  $\sigma(l) = 0$ . This gives  $C_1 = \rho l$ . Therefore, the stress distribution is  $\sigma = \rho(l-x)$ . The total weight of the plate is  $W = \rho A l$  and the stress at the left end ( $x=0$ ) is  $\sigma(0) = \rho l$ .

above can be shown as follows:



Below figure of stress distribution of stress

from theory of elasticity:

$$\sigma = \frac{E}{1-\mu} \epsilon$$

In the stress strain curve,

$$\epsilon = \frac{\sigma}{E}$$



Hence, Eq. 1 changes to,

$$\sigma_{\max} = -\sigma_{\min} = \frac{E}{1+\mu} (\epsilon_{\max}) \quad \text{Eq. 2}$$

In regard to the shearing stresses and strains,

$$\tau_{\max} = G \gamma_{\max}$$

$$G = \frac{E}{2(1+\mu)}$$

$$\frac{\gamma_{\max}}{2} = \epsilon_{\max}$$

Hence,

$$\tau_{\max} = \frac{E}{(1+\mu)} \epsilon_{\max} = \sigma_{\max} \quad \text{Eq. 3}$$

Since the above development considers the material tested as homogeneous, appropriate values of  $E$  and  $\mu$  must be chosen. The problem then is to install an adequate strain gage radially at a  $45^\circ$  angle through the thickness of the Metalite plate at the point the stress is desired to be found.

These gages were placed as near the circumferential boundary as possible so that a maximum reading would be obtained. A comparison could then be made to the loading equation for shear, i.e.:

$$\tau = \frac{p \pi r^2}{2 \pi r t_c} \quad \text{Eq. 4}$$

where

$p$  = normal load, psi.  
 $r$  = radius, in.  
 $t_c$  = core thickness, in.

The theory involving the minor issues, i.e., the panel deflection curve and the stresses in the metal faces

where,  $\mu = 1$  for steel,  $\mu = 2$  for copper,  $\mu = 3$  for brass,  $\mu = 4$  for aluminum,  $\mu = 5$  for iron,  $\mu = 6$  for lead,  $\mu = 7$  for zinc,  $\mu = 8$  for tin,  $\mu = 9$  for silver,  $\mu = 10$  for gold,  $\mu = 11$  for platinum,  $\mu = 12$  for nickel,  $\mu = 13$  for cobalt,  $\mu = 14$  for manganese,  $\mu = 15$  for chromium,  $\mu = 16$  for vanadium,  $\mu = 17$  for niobium,  $\mu = 18$  for molybdenum,  $\mu = 19$  for tungsten,  $\mu = 20$  for tantalum,  $\mu = 21$  for niobium,  $\mu = 22$  for molybdenum,  $\mu = 23$  for tungsten,  $\mu = 24$  for tantalum,  $\mu = 25$  for niobium,  $\mu = 26$  for molybdenum,  $\mu = 27$  for tungsten,  $\mu = 28$  for tantalum,  $\mu = 29$  for niobium,  $\mu = 30$  for molybdenum,  $\mu = 31$  for tungsten,  $\mu = 32$  for tantalum,  $\mu = 33$  for niobium,  $\mu = 34$  for molybdenum,  $\mu = 35$  for tungsten,  $\mu = 36$  for tantalum,  $\mu = 37$  for niobium,  $\mu = 38$  for molybdenum,  $\mu = 39$  for tungsten,  $\mu = 40$  for tantalum,  $\mu = 41$  for niobium,  $\mu = 42$  for molybdenum,  $\mu = 43$  for tungsten,  $\mu = 44$  for tantalum,  $\mu = 45$  for niobium,  $\mu = 46$  for molybdenum,  $\mu = 47$  for tungsten,  $\mu = 48$  for tantalum,  $\mu = 49$  for niobium,  $\mu = 50$  for molybdenum,  $\mu = 51$  for tungsten,  $\mu = 52$  for tantalum,  $\mu = 53$  for niobium,  $\mu = 54$  for molybdenum,  $\mu = 55$  for tungsten,  $\mu = 56$  for tantalum,  $\mu = 57$  for niobium,  $\mu = 58$  for molybdenum,  $\mu = 59$  for tungsten,  $\mu = 60$  for tantalum,  $\mu = 61$  for niobium,  $\mu = 62$  for molybdenum,  $\mu = 63$  for tungsten,  $\mu = 64$  for tantalum,  $\mu = 65$  for niobium,  $\mu = 66$  for molybdenum,  $\mu = 67$  for tungsten,  $\mu = 68$  for tantalum,  $\mu = 69$  for niobium,  $\mu = 70$  for molybdenum,  $\mu = 71$  for tungsten,  $\mu = 72$  for tantalum,  $\mu = 73$  for niobium,  $\mu = 74$  for molybdenum,  $\mu = 75$  for tungsten,  $\mu = 76$  for tantalum,  $\mu = 77$  for niobium,  $\mu = 78$  for molybdenum,  $\mu = 79$  for tungsten,  $\mu = 80$  for tantalum,  $\mu = 81$  for niobium,  $\mu = 82$  for molybdenum,  $\mu = 83$  for tungsten,  $\mu = 84$  for tantalum,  $\mu = 85$  for niobium,  $\mu = 86$  for molybdenum,  $\mu = 87$  for tungsten,  $\mu = 88$  for tantalum,  $\mu = 89$  for niobium,  $\mu = 90$  for molybdenum,  $\mu = 91$  for tungsten,  $\mu = 92$  for tantalum,  $\mu = 93$  for niobium,  $\mu = 94$  for molybdenum,  $\mu = 95$  for tungsten,  $\mu = 96$  for tantalum,  $\mu = 97$  for niobium,  $\mu = 98$  for molybdenum,  $\mu = 99$  for tungsten,  $\mu = 100$  for tantalum.

$$\sigma = \frac{F}{A} = \frac{W}{A} = \frac{mg}{A}$$

in terms of the material properties and geometry.

$$\sigma = \frac{F}{A} = \frac{W}{A} = \frac{mg}{A}$$

$$\sigma = \frac{F}{A} = \frac{W}{A} = \frac{mg}{A}$$

$$\sigma = \frac{F}{A} = \frac{W}{A} = \frac{mg}{A}$$

$$\sigma = \frac{F}{A} = \frac{W}{A} = \frac{mg}{A}$$

where the above relationship connects the material  
 properties, geometry, and the weight of the mass.  
 The purpose of this is to illustrate the behavior of the  
 system under a given load. The behavior of the  
 material plate of the system is shown to be linear.  
 These data were taken as part of the experimental  
 work. It is possible to find a maximum value for the  
 system. A comparison with the data for the loading  
 equation is shown, i.e.,

$$\sigma = \frac{F}{A} = \frac{W}{A} = \frac{mg}{A}$$

$\sigma$  = normal stress, psi.  
 $F$  = force, lb.  
 $A$  = area, in.<sup>2</sup>  
 $W$  = weight, lb.  
 $m$  = mass, lb.  
 $g$  = acceleration, ft./sec.<sup>2</sup>

The above equation for stress is valid for the  
 case of uniform stress and strain in the material.

is taken up in Appendix A.

This investigation was carried out during the school year of 1948-1949 at the University of Minnesota, under the supervision of Prof. J. A. Wise, thesis adviser.



This investigation was carried out during the

Abstracts of 1980-1981 at the University of Minnesota, 1981

ALL INFORMATION CONTAINED HEREIN IS UNCLASSIFIED

## TESTING EQUIPMENT AND PROCEDURE

The Metalite circular panel tested was a product of Chance Vought Aircraft, Dallas, Texas. It had the following characteristics:

- (1) Size - Diameter, 30 in.  
Outside average thickness, 0.26 in.
- (2) Core - End grain balsa. Density, 9 lb. per cu. ft.  $4\frac{1}{2}$   
-0  
Thickness of core, 0.23 in.
- (3) Faces- 0.012 in. 75S-T6 alclad, grain of opposite faces parallel.
- (4) Adhesive - Redux.

The plate had an initial domed curvature of 1/8 inch at the center.

The testing apparatus is shown in Fig. 1. A two inch thick, forty-two inch diameter circular flat steel plate was used as a base. To this base was secured a support ring made of one inch aluminum angle which had been bent on a metal shrinker to the shape of a 14-5/8 in. radius ring. The top of this angle was beaded (3/16 in. dia.) allowing minimum contact area between the support and test plate. Sealing putty was used outside the bead to assure airtightness.

By means of an aspirator, operating off from an air pressure line, air was withdrawn from the area beneath the test panel through a small hole drilled through the base plate. A second hose line from this base plate opening led to a mercury manometer, which was open to the atmosphere. By





means of a suitable scale the plate loading could be directly observed at the manometer.

Five Ames dial deflection gages were placed radially as shown in Figs. 1 and 3. Baldwin rosette strain gages were placed on the top and lower faces as shown in Fig. 3. Small holes were drilled through the vertical web of angle support to carry out the wire leads from the under side strain gages.

The special single wire strain gages (See Appendix B), set radially at a  $45^\circ$  angle through the core, were placed in pairs around the circumference of the test plate as shown in Fig. 2. These gages had been installed by first drilling a  $45^\circ$  hole through the thickness of the panel with a #70 (0.028 in. dia.) drill. A one and one-half to two inch length of the one mil gage wire (furnished by Baldwin Southwark), was threaded through the hole. Bonding glue was introduced into the hole by means of a #250 hypodermic needle and syringe, great care being exercised as the needle was moved up and down along the wire in the hole. A small amount of tension was kept on the wire during the drying process to prevent kinks and waviness. When dry, the cement acts as an insulator for the gage wire as it passes the aluminum faces. The exposed external ends of the wire were then soldered to the "X"-Box lead wires.

Use was made of the standard SX-4 Baldwin "X"-Box, the strains being read directly in micro-inches per inch. A Gage Factor of 2.00 was used for the single wire strain gages

RECEIVED AT ALBANY OFFICIALS - 1944

1965

since their Gage Factor of 1.31 could not be accommodated on the "K"-Box. (See Results and Discussion for Gage Factor correction method).

Since these single wire gages, including the dummy gage, lacked standardization in respect to length and ohms resistance, they could not all be balanced with the dummy gage on the "K"-Box. Their resistances varied from 26.2 ohms to a maximum of 57.4 ohms for the dummy gage. By placing a slide wire potentiometer in parallel with the dummy gage its resistance could be cut down to match the others and the "K"-Box could be balanced.

The testing procedure was standard for obtaining the rosette and Ames dial readings. One quarter psi. loading increments up to one and one-quarter psi were used. All gages zeroed to their original settings at the end of the tests.

The same loads were used for the single wire gages but the load was released after each reading, the zero setting checked. A loading sequence was carried through completely with one gage before moving to the next one, thereby avoiding repeated heating and cooling of the potentiometer coils. Until this potentiometer became thoroughly heated, the resulting change in resistance was very noticeable as a continual creep of the needle across the strain scale. In general, runs were not started unless the creep had dropped to less than ten micro-inches per minute with adjustments being made when



also their own view of the world and by themselves  
 the world. (The world is not the world of the world.)  
 the world is the world.

— The world is the world, the world is the world.

— The world is the world, the world is the world.

— The world is the world, the world is the world.

— The world is the world, the world is the world.

— The world is the world, the world is the world.

— The world is the world, the world is the world.

— The world is the world, the world is the world.

— The world is the world, the world is the world.

— The world is the world, the world is the world.

— The world is the world, the world is the world.

— The world is the world, the world is the world.

— The world is the world, the world is the world.

— The world is the world, the world is the world.

— The world is the world, the world is the world.

— The world is the world, the world is the world.

— The world is the world, the world is the world.

— The world is the world, the world is the world.

— The world is the world, the world is the world.

— The world is the world, the world is the world.

— The world is the world, the world is the world.

— The world is the world, the world is the world.

— The world is the world, the world is the world.

— The world is the world, the world is the world.

necessary for advance of the zero setting.

Due to the nature of the investigation, repeated runs were made on each single wire strain gage.

[illegible]

1960-1961

## RESULTS AND DISCUSSION

## I. Shear Stresses (Single Wire 45° Strain Gages)

Since the main objective of this project was to perfect and prove this method of testing, great care was taken in obtaining the strain readings (Tables I through V) of the single wire gages. Each reading was taken individually, that is, the air load was released after each reading and the zero setting of the "K"-Box checked. Repeated runs were made to determine if there was any slippage or creep in the gage itself. Gage #6A, Table 4, may have been a case where slippage occurred between the first two runs and the last four. Two of the gages, #2 and #12, were broken accidentally before repeated runs could be made.

The best average was calculated for each set of runs and was plotted with all points being shown (Fig. 4 through 9). Since the Gage Factor, 1.31, of the single wire gages, (See Appendix B), could not be accommodated on the "K"-Box, an arbitrary Gage Factor of 2.00 was used. The best average runs were then corrected to the Gage Factor of 1.31 as follows:

$$\epsilon_{(\text{corrected})} = \epsilon_{(\text{as read})} \times \frac{2.00}{1.31}$$

These final corrected values are plotted for comparison in Fig. 10. It will be noted that Gages #4 and #6A show the closest semblance of duplication. It is assumed then, for lack of better data, that their average at 1-1/4 psi, of 190 micro-inches per inch is a bonafide value. Then





by use of Eq. 3 above, on page 4, the shearing stress can be determined.

The value of  $E$  for use here was selected as 250,000 psi, and  $\mu$  as 0.36 (ref. 5 and 6). Inserting these and  $\epsilon_{\max}$  of 190 in Eq. 3 gives:

$$\tau = \frac{E}{(1+\mu)} \epsilon_{\max}$$

$$\tau = \frac{250,000}{(1+0.36)} \times \frac{190}{10^6}$$

$$\tau = 35 \text{ psi.}$$

For comparison, Eq. 4, page 4, gives:

$$\tau = \frac{pR}{2t} = \frac{1.25 \times 14.625}{2 \times .23}$$

$$\tau = 39.8 \text{ psi.}$$

The stress value calculated from the experimental results should be considered with caution due to the three variables involved in its computation; namely,  $\epsilon_{\max}$ ,  $E$ , and  $\mu$ .  $E$  may vary from 10,000 psi tangentially to 450,000 psi parallel to the wood grain. Likewise, the six values of Poisson's Ratio for balsa vary from 0.009 to 0.36, depending upon the plane of the stresses under consideration. A different value of  $E$  could have varied the result considerably. Hence before this testing method, once perfected, could be of value, a more rigorous determination of the characteristics,  $E$  and  $\mu$ , must be accomplished.

Although the  $\epsilon_{\max}$  used above was approximately the largest obtained, there is no indication that it is a true

of the 1000 ft. level, the 1000 ft. level is the 1000 ft. level.

The 1000 ft. level is the 1000 ft. level. The 1000 ft. level is the 1000 ft. level.

$$\frac{1000}{1000} = \frac{1000}{1000} \quad 5$$

$$\frac{1000}{1000} = \frac{1000}{1000} \quad 5$$

$$\frac{1000}{1000} = \frac{1000}{1000} \quad 5$$

$$\frac{1000}{1000} = \frac{1000}{1000} \quad 5$$

$$\frac{1000}{1000} = \frac{1000}{1000} \quad 5$$

$$\frac{1000}{1000} = \frac{1000}{1000} \quad 5$$

The 1000 ft. level is the 1000 ft. level.

The 1000 ft. level is the 1000 ft. level.

The 1000 ft. level is the 1000 ft. level.

The 1000 ft. level is the 1000 ft. level.

The 1000 ft. level is the 1000 ft. level.

The 1000 ft. level is the 1000 ft. level.

The 1000 ft. level is the 1000 ft. level.

The 1000 ft. level is the 1000 ft. level.

The 1000 ft. level is the 1000 ft. level.



reading. As can be seen on Fig. 10, very little duplication of readings between corresponding gages was attained. For instance, there is considerable spread among the values of the tension gages, with a still greater difference found for the compression gages. Further, it was expected that the compression-tension mates (i.e., #1 & 2, #3 & #4, etc.) would be numerically equal but of opposite sign. Gages #1 and #2 and #3A and #4 show some equality as mates but on the other hand they do not cross-check, i.e., #1 and #3, and #2 and #4.

Gage #3A's position could be strengthened if the straight line curve of #1 and #11 were extended to cross the vertical axis and then the two curves moved positively and parallel-to their present position until they were zeroed on the origin. Here again, though, #3A does not agree closely with any of the compression gages as expected.

Three factors that may have effected these results could be:

- (1) The initial curvature of the plate.
- (2) The fact that simple support was not completely realized, due to friction between the lower panel face and the support, thereby creating a longitudinal force in the lower face.
- (3) The fact that precise loading was limited by the use of a mercury manometer.

Despite the fact that complete success of the method was not realized, it was encouraging to finally get the correct and definite indications of tension and especially compression. It is believed that this method of test



(1) The first question is whether the  
 evidence is sufficient to establish the  
 fact of the commission of the crime.  
 (2) The second question is whether the  
 evidence is sufficient to establish the  
 fact of the commission of the crime.  
 (3) The third question is whether the  
 evidence is sufficient to establish the  
 fact of the commission of the crime.  
 (4) The fourth question is whether the  
 evidence is sufficient to establish the  
 fact of the commission of the crime.  
 (5) The fifth question is whether the  
 evidence is sufficient to establish the  
 fact of the commission of the crime.  
 (6) The sixth question is whether the  
 evidence is sufficient to establish the  
 fact of the commission of the crime.  
 (7) The seventh question is whether the  
 evidence is sufficient to establish the  
 fact of the commission of the crime.  
 (8) The eighth question is whether the  
 evidence is sufficient to establish the  
 fact of the commission of the crime.  
 (9) The ninth question is whether the  
 evidence is sufficient to establish the  
 fact of the commission of the crime.  
 (10) The tenth question is whether the  
 evidence is sufficient to establish the  
 fact of the commission of the crime.

still has possibilities for further investigation. The main difficulty is concerned with obtaining a reliable bond between the core material and the complete length of the wire gage. The only glue tried was DuPont Cement #5458, ordinarily used with the Baldwin electrical strain gages. It is believed that once the glue had dried that the bond between the wire and the balsa was a permanent one (except for the possibility of #6A) since the same results were obtainable on repeated runs. However, whether the whole gage was included in this bond is not definite.

Other improvements could be made without too great difficulty by correcting the three factors mentioned two paragraphs above. Also it is suggested that the gages be moved radially inward from the support. It may be that stress concentrations from the contact area of the support were the reason for failure of the strain of the mated wires to coincide. The writer used a clearance from the support to the wire opening on the face of  $1\frac{1}{2}$  the thickness of the plate.

A size 75 drilled hole (.021 in.) in the core, for threading the single wire gage, may give adequate gluing room and make a snugger fit for the wire. The #50 (.0135 in) drill originally used did not allow for ample passage of the glue while the #70 (.028 in.) drill finally used may have been too large.

One final improvement would be to make certain that the gage wire is perfectly straight when bonded. Otherwise a

The first important point is that the data are not normally distributed. This is evident from the fact that the distribution is skewed to the right, with a long tail of high values. This suggests that the data may be better described by a log-normal distribution. To test this, we can take the natural logarithm of the data and check if the resulting distribution is approximately normal. If it is, then the original data are log-normally distributed.



subnormal tension reading will result as the kinks and slack are being taken up and absorbed with the loading.

## II. Deflection and Face Stresses

The deflection data as taken with the Ames dial gages (Table VI and Fig. 13) appears reliable. However, the one-quarter pound loading increments are not precise values although they were adequate for purposes of this test. When using such low pressure values, an alcohol manometer would have been more accurate.

From the development of the deflection equation in Appendix A, it is seen that the additional deflection due to shear deformation is practically negligible in the thin panel tested, even though shear stresses were present.

Two theoretical deflection curves (effect due to shear deformation not included) are plotted on Fig. 13 with the test deflection curves. While fairly close agreement is found for the  $1/4$  psi curve, a large difference is noticed for the  $1-1/4$  psi loading curve. It is believed that this discrepancy is due almost entirely to the support friction factor mentioned on page 12. An increase in normal load would increase the effect of the longitudinal load and the plate deflection would tend to be less. The strains as obtained from the rosettes were converted to principal stresses by use of Ref. 7 (See Tables VII, VIII, and IX, and Figs. 11 and 12). The readings and results are believed to be accurate and reliable.



THE ABOVE INFORMATION WAS OBTAINED FROM THE FILES OF THE  
FEDERAL BUREAU OF INVESTIGATION AND IS BEING FURNISHED TO YOU  
FOR YOUR INFORMATION. IT IS REQUESTED THAT YOU KEEP THIS INFORMATION  
CONFIDENTIAL AND NOT DISCLOSE IT TO ANY OTHER PERSONS.  
YOUR COOPERATION IN THIS MATTER IS APPRECIATED.

## CONCLUSIONS

(1) This single wire gage method of test for determining shearing stresses shows positive signs of workability. However, its validity and reliability can not yet be accepted until present results are substantiated by further investigation.

(2) Tests are also needed to establish suitable core values of  $E$  and  $\mu$  to be used in conjunction with this test procedure.

(3) The results obtained herein were materially effected both by the original inherent curvature of the plate and the fact that simply supported conditions were not realized.

# CONCLUSIONS

(i) This study has been carried out over the  
 following period: 1950-1951. The results of the  
 investigation, however, are not yet available and  
 will be published in a separate report at a later  
 date by the author.

(ii) The results of the investigation will  
 be published in a separate report at a later  
 date by the author.

(iii) The results of the investigation will  
 be published in a separate report at a later  
 date by the author.

## APPENDIX A

### THEORY OF FACE STRESSES & DEFLECTION

#### I. Face Stresses

From the theory of elasticity, the equations for stresses in the cross-section of a rectangular plate are:

$$\sigma_x = \frac{Ez}{1-\mu^2} \left[ \frac{\partial^2 f}{\partial x^2} + \mu \frac{\partial^2 f}{\partial y^2} \right] \quad \text{Eq. A1}$$

$$\sigma_y = \frac{Ez}{1-\mu^2} \left[ \frac{\partial^2 f}{\partial y^2} + \mu \frac{\partial^2 f}{\partial x^2} \right]$$

$f$  = deflection.  
 $z$  = vertical distance from neutral axis to stress point.

Converted to polar coordinates and a circular plate, the stress equations are:

$$\sigma_t = \frac{Ez}{1-\mu^2} \left[ \frac{1}{r} \frac{\partial f}{\partial r} + \mu \frac{\partial^2 f}{\partial r^2} \right] \quad \text{Eq. A2}$$

$$\sigma_r = \frac{Ez}{1-\mu^2} \left[ \frac{\partial^2 f}{\partial r^2} + \frac{\mu}{r} \frac{\partial f}{\partial r} \right] \quad \text{Eq. A3}$$

Applying the LaGrange equation for the deflection,  $f$ , and a loading,  $p$ , it can be shown (ref.8) that for the circular plate,

$$f = Ar^2 + C + \frac{pr^4}{64N} \quad \text{Eq. A4}$$

where,

$r$  = radius  
 $N$  = flexural stiffness.

Substituting in Eq. A3,

$$\sigma_r = \frac{Ez}{1-\mu^2} \left[ 2A(1+\mu) + \frac{4pr^2}{64N}(3+\mu) \right] \quad \text{Eq. A5}$$





Applying boundary conditions to Eq. A5,

when  $r = R$ ,  $\sigma_r = 0$  -

$$A = - \frac{2pR^2}{64N} \times \frac{3+\mu}{1+\mu} \quad \text{Eq. A6}$$

Applying boundary conditions to Eq. A4,

when  $r = R$ ,  $J = 0$ ,

$$C = \frac{pR^4}{64N} \times \frac{5+\mu}{1+\mu} \quad \text{Eq. A7}$$

Thus for outer fibre, top face, Eq. A5 becomes,

(See Fig. 2 for symbols)

$$\sigma_r = - \frac{E_f(h_c + 2t_f)p}{2(1-\mu^2)64N} [(3+\mu)(R^2 - r^2)] \quad \text{Eq. A8}$$

$$\text{Let}_{(1)} N = \frac{E_f t_f A^2}{2(1-\mu^2)}$$

$$\sigma_r = - \frac{(h_c + 2t_f)p}{16t_f h^2} [(3+\mu)(R^2 - r^2)] \quad \text{Eq. A9}$$

Applying Eq. A9 to the plate tested, where,

$$E = 10^7 \text{ psi} \quad \mu = \frac{1}{3}$$

$$h_c = 0.236 \text{ in (0.23" balsa core plus rubber bond)}$$

$$t_f = 0.012 \text{ in.} \quad h = h_c + t_f = 0.248 \text{ in.}$$

$$\sigma_r = 73.4 p (r^2 - R^2) \quad \text{Eq. 10}$$

(1) Seide, Paul and Stowell, E.Z.; Elastic and Plastic Buckling of Simply Supported Metalite Type Sandwich Plates, NACA Tech. Note 1822, February 1949.



Taking the point of rosettes #2 and #3, where the radius is 7.3125 inches and using a loading of 0.25 psi.,

$$\sigma_r = \pm 2943 \text{ psi.}$$

This shows fair agreement with test results of Tables VIII and IX, page 33 and 34, where values are,

$$\sigma_r \cong -2823 \text{ psi, compression (top face)}$$

$$\sigma_r \cong +2575 \text{ psi Tension (lower face)}$$

At 0.50 psi. load, calculated gives,

$$\sigma_r = \pm 5,885 \text{ psi}$$

while test shows,

$$\sigma_r \cong -4230 \text{ psi}$$

$$\sigma_r \cong +4840 \text{ psi}$$

At 0.75 psi., calculated shows,

$$\sigma_r = 8830 \text{ psi.}$$

while tests gave,

$$\sigma_r \cong -5770$$

$$\sigma_r \cong +7650$$

As can be seen the discrepancy between the test results and the analytical results is getting larger with increased load due to the failure to achieve a simple support. The effects of the inherent longitudinal load are increasing with the load.





## II. DEFLECTION

To obtain the deflection equation (no shear deformation) apply the constants A and C, Equations A6 and A7 to the deflection Equation A4, giving,

$$\delta = \frac{P}{64N} \left[ r^4 - 2 \frac{3+\mu}{1+\mu} (r^2 R^2) + \frac{5+\mu}{1+\mu} R^4 \right] \quad \text{Eq. A11}$$

Applying the constant test plate values to Eq. A11, the following deflection equation is obtained,

$$\delta = 0.000003767 P [r^4 - 1070 r^2 + 183,200] \quad \text{Eq. A12}$$

or at the center,

$$\delta = 0.690 P \quad \text{Eq. A13}$$

Considering deflections due to shear as found in reference 9, page 143, but using a constant cross-section value instead of a parabolic curve, the shear deflection is,

$$\delta_{\text{shear}} = \frac{1}{4} \frac{P}{G h} (R^2 - r^2) \quad \text{Eq. A14}$$

Using a shear modulus for Metalite of this core and face of  $G = 29,000 \text{ psi}$ . from reference 5, Fig. 4.01, at the center Eq. A14 gives,

$$\delta_{\text{shear}} = 0.00674 P$$

Total center deflection will be,

$$\begin{aligned} \delta &= (0.690 + 0.00674) P \\ &= 0.69674 P \end{aligned}$$

Or, in the case of the thin panel tested, the deflection due to shear is only 0.98% of the total, or just less than one percent.



Neglecting this negligible shear deflection and considering Eq. All alone, the following values for  $\delta$  are found for the 0.25 psi., the 1.00 psi., and the 1.25 psi. loading -

Table of Deflections

Radius(in.)	Loading(psi)		
	0.25	1.00	1.25
0	0.1725	0.690	0.803
3.75	0.1588	0.635	0.794
6.3125	0.1337	0.535	0.609
10.00	0.0813	0.325	0.400





## APPENDIX B

Problems Concerning the Use of the Single  
Wire Strain Gage

Numerous difficulties were encountered in attempting to perfect the installation of the single wire strain gage for use in this testing method. The greatest of these was obtaining a complete and reliable bond between the wire and the core material.

As mentioned in the body of this report, a 0.0135 inch hole was first tried as a conduit through the core for the gage. After the gage wire was threaded through the hole, glue was placed over the opening on each face of the panel. The wire was then slowly drawn back and forth through the core so that the glue would be carried in through the length of the conduit. However, loading tests indicated that insufficient glue was reaching the interior, since all gages slipped with the first loading.

An attempt was made to correct this difficulty by heating the gage wire which in turn would heat and loosen the glue into better distribution. Heating was attempted by passing current through the wire, but it did not prove at all practical, the wire gages being too delicate. Another, to draw the glue through the core, was then tried on the 0.0135 inch hole. In this case, the quick-drying glue would start hardening as soon as it reached the opposite face, thereby blocking the passage of sufficient glue for

...and the ...

— *Journal of the American Medical Association*, 1964, 191: 1000-1001.

and the same method.

1987, 1988, 1989, 1990, 1991, 1992, 1993, 1994, 1995, 1996, 1997, 1998, 1999, 2000, 2001, 2002, 2003, 2004, 2005, 2006, 2007, 2008, 2009, 2010, 2011, 2012, 2013, 2014, 2015, 2016, 2017, 2018, 2019, 2020, 2021, 2022, 2023, 2024, 2025, 2026, 2027, 2028, 2029, 2030, 2031, 2032, 2033, 2034, 2035, 2036, 2037, 2038, 2039, 2040, 2041, 2042, 2043, 2044, 2045, 2046, 2047, 2048, 2049, 2050, 2051, 2052, 2053, 2054, 2055, 2056, 2057, 2058, 2059, 2060, 2061, 2062, 2063, 2064, 2065, 2066, 2067, 2068, 2069, 2070, 2071, 2072, 2073, 2074, 2075, 2076, 2077, 2078, 2079, 2080, 2081, 2082, 2083, 2084, 2085, 2086, 2087, 2088, 2089, 2090, 2091, 2092, 2093, 2094, 2095, 2096, 2097, 2098, 2099, 2100, 2101, 2102, 2103, 2104, 2105, 2106, 2107, 2108, 2109, 2110, 2111, 2112, 2113, 2114, 2115, 2116, 2117, 2118, 2119, 2120, 2121, 2122, 2123, 2124, 2125, 2126, 2127, 2128, 2129, 2130, 2131, 2132, 2133, 2134, 2135, 2136, 2137, 2138, 2139, 2140, 2141, 2142, 2143, 2144, 2145, 2146, 2147, 2148, 2149, 2150, 2151, 2152, 2153, 2154, 2155, 2156, 2157, 2158, 2159, 2160, 2161, 2162, 2163, 2164, 2165, 2166, 2167, 2168, 2169, 2170, 2171, 2172, 2173, 2174, 2175, 2176, 2177, 2178, 2179, 2180, 2181, 2182, 2183, 2184, 2185, 2186, 2187, 2188, 2189, 2190, 2191, 2192, 2193, 2194, 2195, 2196, 2197, 2198, 2199, 2200, 2201, 2202, 2203, 2204, 2205, 2206, 2207, 2208, 2209, 2210, 2211, 2212, 2213, 2214, 2215, 2216, 2217, 2218, 2219, 2220, 2221, 2222, 2223, 2224, 2225, 2226, 2227, 2228, 2229, 2230, 2231, 2232, 2233, 2234, 2235, 2236, 2237, 2238, 2239, 2240, 2241, 2242, 2243, 2244, 2245, 2246, 2247, 2248, 2249, 2250, 2251, 2252, 2253, 2254, 2255, 2256, 2257, 2258, 2259, 2260, 2261, 2262, 2263, 2264, 2265, 2266, 2267, 2268, 2269, 2270, 2271, 2272, 2273, 2274, 2275, 2276, 2277, 2278, 2279, 2280, 2281, 2282, 2283, 2284, 2285, 2286, 2287, 2288, 2289, 2290, 2291, 2292, 2293, 2294, 2295, 2296, 2297, 2298, 2299, 2300, 2301, 2302, 2303, 2304, 2305, 2306, 2307, 2308, 2309, 2310, 2311, 2312, 2313, 2314, 2315, 2316, 2317, 2318, 2319, 2320, 2321, 2322, 2323, 2324, 2325, 2326, 2327, 2328, 2329, 2330, 2331, 2332, 2333, 2334, 2335, 2336, 2337, 2338, 2339, 2340, 2341, 2342, 2343, 2344, 2345, 2346, 2347, 2348, 2349, 2350, 2351, 2352, 2353, 2354, 2355, 2356, 2357, 2358, 2359, 2360, 2361, 2362, 2363, 2364, 2365, 2366, 2367, 2368, 2369, 2370, 2371, 2372, 2373, 2374, 2375, 2376, 2377, 2378, 2379, 2380, 2381, 2382, 2383, 2384, 2385, 2386, 2387, 2388, 2389, 2390, 2391, 2392, 2393, 2394, 2395, 2396, 2397, 2398, 2399, 2400, 2401, 2402, 2403, 2404, 2405, 2406, 2407, 2408, 2409, 2410, 2411, 2412, 2413, 2414, 2415, 2416, 2417, 2418, 2419, 2420, 2421, 2422, 2423, 2424, 2425, 2426, 2427, 2428, 2429, 2430, 2431, 2432, 2433, 2434, 2435, 2436, 2437, 2438, 2439, 2440, 2441, 2442, 2443, 2444, 2445, 2446, 2447, 2448, 2449, 2450, 2451, 2452, 2453, 2454, 2455, 2456, 2457, 2458, 2459, 2460, 2461, 2462, 2463, 2464, 2465, 2466, 2467, 2468, 2469, 2470, 2471, 2472, 2473, 2474, 2475, 2476, 2477, 2478, 2479, 2480, 2481, 2482, 2483, 2484, 2485, 2486, 2487, 2488, 2489, 2490, 2491, 2492, 2493, 2494, 2495, 2496, 2497, 2498, 2499, 2500, 2501, 2502, 2503, 2504, 2505, 2506, 2507, 2508, 2509, 2510, 2511, 2512, 2513, 2514, 2515, 2516, 2517, 2518, 2519, 2520, 2521, 2522, 2523, 2524, 2525, 2526, 2527, 2528, 2529, 2530, 2531, 2532, 2533, 2534, 2535, 2536, 2537, 2538, 2539, 2540, 2541, 2542, 2543, 2544, 2545, 2546, 2547, 2548, 2549, 2550, 2551, 2552, 2553, 2554, 2555, 2556, 2557, 2558, 2559, 2560, 2561, 2562, 2563, 2564, 2565, 2566, 2567, 2568, 2569, 2570, 2571, 2572, 2573, 2574, 2575, 2576, 2577, 2578, 2579, 2580, 2581, 2582, 2583, 2584, 2585, 2586, 2587, 2588, 2589, 2590, 2591, 2592, 2593, 2594, 2595, 2596, 2597, 2598, 2599, 2600, 2601, 2602, 2603, 2604, 2605, 2606, 2607, 2608, 2609, 2610, 2611, 2612, 2613, 2614, 2615, 2616, 2617, 2618, 2619, 2620, 2621, 2622, 2623, 2624, 2625, 2626, 2627, 2628, 2629, 2630, 2631, 2632, 2633, 2634, 2635, 2636, 2637, 2638, 2639, 2640, 2641, 2642, 2643, 2644, 2645, 2646, 2647, 2648, 2649, 2650, 2651, 2652, 2653, 2654, 2655, 2656, 2657, 2658, 2659, 2660, 2661, 2662, 2663, 2664, 2665, 2666, 2667, 2668, 26

[illegible]

of violence with respect to the use of force in the

There is a very strong possibility that the information in this document is being disseminated to unauthorized persons. If you are not an authorized recipient, please do not read, copy, or distribute this information. If you are an authorized recipient, please do not discuss the contents of this document with unauthorized persons. If you have any questions, please contact the appropriate authority.

bonding. A change to a larger hole, 0.035 inch, corrected this trouble, but still not enough of the glue was being distributed inside for satisfactory bonding purposes.

The most satisfactory gluing method tried and the one the final results were obtained from, was to employ a hypo needle to introduce the glue into the gage hole, as mentioned earlier in the report. Positive results were obtained in all cases, although very weak in some instances. A re-gluing of these weak ones showed marked improvement, the old bond being loosened with a hypo injected solvent (acetone). Although this last method gave partial success it can not be accepted until better duplication of results is obtained.

Another problem mentioned in the report is the desirability of having all the single wire gages of the same resistance, or within a few ohms, of the dummy gage, thus eliminating the use of the potentiometer or additional resistance.

The exposed portions of the gage wire should be shielded from drafts since sudden temperature changes make a noticeable effect on strain readings being taken from the "K"-Box.

Since the Gage Factor, needed for use with the "K"-Box, of this single gage wire was unknown, it had to be determined. The Gage Factor is a constant for each type and size of wire and is:



standing, a change to a higher class, 5,000 foot, surrounded  
 from the north, but still not enough of the glass was being  
 applied to the south for satisfactory building purposes.  
 The most satisfactory thing about the glass was the  
 way the glass panels were obtained from, and in making a  
 type which is important in the glass industry, and  
 considered useful in the report. The glass panels were ob-  
 tained in all cases, although very much in some instances.  
 A reference to the glass was made in some cases, however,  
 the old glass being found to be in some instances better  
 (better). Although the glass had been given better results  
 it was not so satisfactory as the other specimens of the glass  
 as obtained.  
 Another problem mentioned in the report is the  
 desirability of having all the glass with some of the  
 same thickness, or within a few feet, of the same size,  
 this eliminated the use of the specimens of different  
 thicknesses.  
 The report further at the end of the report is  
 obtained from the glass which was made in some cases  
 a reference to the glass which was made from the  
 "A" glass, which was made from the glass which was  
 from the glass which was made from the glass which was  
 "B" glass, at the glass which was made from the glass which  
 of the glass. The glass which was made from the glass which  
 was made of the glass and the glass which was made from the

$$G.F. = \frac{\frac{\Delta R}{R}}{\frac{\Delta L}{L}}$$

Since it was impractical to measure these factors for the wire concerned, the following means was employed. A one-wire paper-covered strain gage was made up on a steel rod whose loading-strain curve was known. Following the pattern of the standard gages, this special one was made by first gluing a piece of rice paper to the rod and then stretching a length of the wire longitudinally over the paper. More glue was applied and a top cover of rice paper placed over all.

When the gage was dry, the "K"-Box leads were soldered to the exposed ends and the rod was then tested in tension in a Michle Testing Machine. Three arbitrary Gage Factor settings were used on three loading runs (Table X).

From the plotted results (Fig. 14), the Gage Factor of the wire gage under test was determined by comparing the three test curves to the known strain curve, the relationship being a direct proportion.

Thus,

$$\text{Run 1} \quad G.F. = \frac{880}{1200} \times 1.77 = 1.30$$

$$\text{Run 2} \quad G.F. = \frac{780}{1200} \times 2.04 = 1.33$$

$$\text{Run 3} \quad G.F. = \frac{710}{1200} \times 2.00 = 1.20$$

$$\text{Average} \quad 1.31$$

Hence, the G.F. for this case is 1.31.

$$\frac{\Delta}{\Delta} = 1.0$$

Since it was impossible to obtain these results for the two measured, but following them are expected, a separate factor-estimated with each one as a result of these factor-estimated results was found. Following the system of the standard theory, each equation was used to find the value of the first factor for the two and then extended a factor of the two factor-estimated over the paper. Each time the system was a step count of this paper found over all.

That the given was 100, the 100-100 factor was estimated in the system and the two and then found in factor in a single factor-estimated. These results were found by using the two and then found over (Table 1). Then the factor-estimated (100, 100) was found. Factor of the two factor-estimated was estimated by the factor the given was 100 in the same factor-estimated, the relationship found a single factor-estimated.

$$\text{Row 1: } 1.0 \times 1.0 = 1.00$$

$$\text{Row 2: } 1.0 \times 1.0 = 1.00$$

$$\text{Row 3: } 1.0 \times 1.0 = 1.00$$

$$\text{Row 4: } 1.0 \times 1.0 = 1.00$$

Thus, the 1.0 for each one is 1.00.



## REFERENCES

1. Reissner, Eric: The Effect of Transverse Shear Deformation on the Bending of Elastic Plates. Jour. Appl. Mech., Vol. 12, No. 2, June 1945, pp. A69-A77.
2. March, E. W.: Effects of Shear Deformation in the Core of a Flat Rectangular Sandwich Panel. Rpt. No. 1582, Forest Products Lab., U. S. Dept. Agriculture, May 1948.
3. Libove, Chas., and Batdorf, S. B.: A General Small-Deflection Theory for Flat Sandwich Plates. NACA TN No. 1526, 1948.
4. Koppers, E. J., and Morris, C. E.: Effects of Shear Deformation in the Core of a Flat Rectangular Sandwich Panel Subjected to Uniformly Distributed Load Normal to its Surface - Simply Supported Edges. Rpt. No. 1563-A, Forest Products Laboratory, U. S. Dept. Agriculture, October 1948.
5. Pitman, W. A., and Cleveland, W. B.: Zetalite Strength Data. Chance Vought Aircraft, Report No. 7412, July 30, 1947.
6. Doyle, D. V.: Elastic Properties of (Balsa) Wood. Rpt. No. 1528, Forest Products Laboratory, U. S. Dept. of Agriculture, June 1948.
7. Nise, J. A.: Circles of Strain. Jour. Aero. Sci., Vol. 7, No. 10, Aug. 1940.
8. Föppl, A., and L. Drang and Zwang, 2nd Edition, H. Oldenbourg, Munich, Vol. 1, 1924.
9. Timoshenko, S.: Theory of Plates and Shells. McGraw-Hill Book Company, Inc., 1940.



## Bibliography

1. Balamant, Boris. The Effect of Temperature on the Rate of Growth of *Chironomus tentans*. *Trudy Vsesoyuznogo Nauchnogo Tsentra*, 1957, No. 1, pp. 100-102.
2. Balamant, Boris. The Effect of Temperature on the Rate of Growth of *Chironomus tentans*. *Trudy Vsesoyuznogo Nauchnogo Tsentra*, 1957, No. 1, pp. 100-102.
3. Balamant, Boris, and Gerasimov, A. A. The Effect of Temperature on the Rate of Growth of *Chironomus tentans*. *Trudy Vsesoyuznogo Nauchnogo Tsentra*, 1957, No. 1, pp. 100-102.
4. Balamant, Boris, and Gerasimov, A. A. The Effect of Temperature on the Rate of Growth of *Chironomus tentans*. *Trudy Vsesoyuznogo Nauchnogo Tsentra*, 1957, No. 1, pp. 100-102.
5. Balamant, Boris, and Gerasimov, A. A. The Effect of Temperature on the Rate of Growth of *Chironomus tentans*. *Trudy Vsesoyuznogo Nauchnogo Tsentra*, 1957, No. 1, pp. 100-102.
6. Balamant, Boris, and Gerasimov, A. A. The Effect of Temperature on the Rate of Growth of *Chironomus tentans*. *Trudy Vsesoyuznogo Nauchnogo Tsentra*, 1957, No. 1, pp. 100-102.
7. Balamant, Boris, and Gerasimov, A. A. The Effect of Temperature on the Rate of Growth of *Chironomus tentans*. *Trudy Vsesoyuznogo Nauchnogo Tsentra*, 1957, No. 1, pp. 100-102.
8. Balamant, Boris, and Gerasimov, A. A. The Effect of Temperature on the Rate of Growth of *Chironomus tentans*. *Trudy Vsesoyuznogo Nauchnogo Tsentra*, 1957, No. 1, pp. 100-102.
9. Balamant, Boris, and Gerasimov, A. A. The Effect of Temperature on the Rate of Growth of *Chironomus tentans*. *Trudy Vsesoyuznogo Nauchnogo Tsentra*, 1957, No. 1, pp. 100-102.
10. Balamant, Boris, and Gerasimov, A. A. The Effect of Temperature on the Rate of Growth of *Chironomus tentans*. *Trudy Vsesoyuznogo Nauchnogo Tsentra*, 1957, No. 1, pp. 100-102.

TABLE I  
SINGLE WIRE STRAIN GAGES  
GAGE READINGS (Micro inches)

Gage # 1						
Load psi	1	Run 2	3	4	Best Average	Corrected for Gage Factor
0.00	0	0	0	0	0.0	0.0
0.25	5	2	3	4	3.5	5.3
0.50	20	14	11	20	16.2	24.8
0.75	40	28	30	32	30.0	45.8
1.00	35	43	45	42	43.3	66.1
1.25	55	62	58	58	58.2	89.0

Gage # 2						
0.00	0	Wire			0.0	0.0
0.25	-	was			-	-
0.50	-20	broken			-20.0	-30.8
0.75	-40				-40.0	-61.1
1.00	-50				-50.0	-76.4
1.25	-60				-60.0	-91.6



TABLE II  
SINGLE WIRE STRAIN GAGES  
GAGE READINGS (Micro inches)

Gage # 3							
Load psi	1	2	Run 3	4	5	Best Average	Corrected for Gage Factor
0.00	0	0	0	0		0.0	0.0
0.25	0	2	1	2		1.7	2.6
0.50	3	6	6	6		5.2	7.9
0.75	5	8	0	7		6.7	10.2
1.00	13	11	12	14		12.5	19.1
1.25	18	19	17	20		18.5	28.2
Gage # 3 <sub>A</sub> (Reglued)							
0.00	0	0	0	0		0.0	0.0
0.25	26	20	24	25		23.8	36.4
0.50	31	28	33	30		30.5	46.6
0.75	39	40	40	39		39.5	60.4
1.00	53	60	64	57		58.5	89.4
1.25	80	80	80	84		81.0	123.7
Gage # 4							
0.00	0	0	0	0	0	0.0	0.0
0.25	-50	-27	-42	-33	-36	-37.6	-57.4
0.50	-62	-56	-52	-50	-	-55.0	-84.0
0.75	-76	-90	-90	-73	-80	-81.8	-125.0
1.00	-105	-100	-107	-105	-	-104.2	-159.0
1.25	-112	-124	-137	-118	-112	-120.6	-184.0





TABLE III  
SINGLE WIRE STRAIN GAGES  
GAGE READINGS (Micro inches)

Gage # 5					
Load psi	1	Run 2	3	Best Average	Corrected for Gage Factor
0.00	0	0	0	0.0	0.0
0.25	8	9	-	8.5	13.0
0.50	15	15	-	15.0	22.9
0.75	22	21	-	21.5	32.8
1.00	32	30	-	31.0	47.4
1.25	44	39	40	41.0	62.6
Gage # 6					
0.00	0			0.0	0.0
0.25	-5			-5.0	-7.6
0.50	-8			-8.0	-12.2
0.75	-10			-10.0	-15.3
1.00	-12			-12.0	-18.3
1.25	-13	-13		-13.0	-19.9



TABLE IV  
SINGLE WIRE STRAIN GAGES  
GAGE READINGS (Micro inches)

Load psi	Gage # 6 <sub>A</sub> (# 6 Reglued)				Average 1 & 2	Corrected for Gage Factor
	1	2				
0.00	0	0			0.0	0.0
0.25	-38	-29			-33.0	-50.9
0.50	-58	-48			-53.0	-81.0
0.75	-112	-75			-81.0	-123.8
1.00	-113	-87			-104.0	-158.8
1.25	-140	-120			-130.0	-198.6

Load	Gage # 6 <sub>A</sub> (Continued)					Corrected for Gage Factor
	3	4	5	6	*	
0.00	0	0	0		0.0	0.0
0.25	-31	-33	-32		-32.0	-48.9
0.50	-48	-50	-48		-48.5	-74.1
0.75	-62	-61	-62		-61.7	-95.0
1.00	-78	-75	-80	-72	-76.2	-114.8
1.25	-79	-91	-89	-81	-85.0	-130.0

\* Average of Runs 3, 4, 5, & 6.





TABLE V  
SINGLE WIRE STRAIN GAGES  
GAGE READINGS (Micro inches)

Gage # 10							
Load psi	1	2	Run 3	4	5	Best Average	Corrected for Gage Factor
0.00	0	0	0	0	0	0.0	0.0
0.25	-35	-13	-10	-13	-11	-11.7	-17.9
0.50	-42	-18	-22	-13	-15	-23.2	-35.4
0.75	-110	-112	-120	-115	-	-115.7	-176.7
1.00	-107	-110	-119	-110	-	-113.0	-174.1
1.25	-113	-107	-115	-111	-	-111.0	-168.0
Gage # 11							
0.00	0	0	0	0		0.0	0.0
0.25	-8	-8	-7	-		-7.7	-11.8
0.50	0	0	0	-		0.0	0.0
0.75	11	16	17	18		17.0	26.0
1.00	35	35	36	-		35.3	53.9
1.25	48	49	42	48		48.3	73.7
Gage # 12							
0.00	0	-				0.0	0.0
0.25	-2	-				-2.0	-3.1
0.50	-4	-				-4.0	-6.1
0.75	-7	-				-7.0	-10.7
1.00	-13	-				-13.0	-19.9
1.25	-23	-23				-23.0	-35.2



TABLE VI

## PLATE DEFLECTIONS (Inches)

Load psi	Center	3.75 in. radius	6.3125 in. radius	10.00 in. radius	14.625 in. radius
0.00	0	0	0	0	0
0.25	-0.175	-0.163	-0.138	-0.086	0
0.50	-0.300	-0.278	-0.235	-0.147	0
0.75	-0.410	-0.380	-0.323	-0.200	0
1.00	-0.489	-0.455	-0.387	-0.242	0
1.25	-0.558	-0.520	-0.442	-0.279	0
1.50	-0.624	-0.595	-0.508	-0.318	0

Note: Deflections were taken by means of Ames dials placed above the top face.





TABLE VII  
ROSETTE STRAIN GAGES  
GAGE READINGS (Micro inches)

		Top Face					
Rosette No.	Gage No.	Strain Readings For Each Loading Increment					
		0 psi	$\frac{1}{4}$ psi	$\frac{1}{2}$ psi	$\frac{3}{4}$ psi	1 psi	$1\frac{1}{4}$ psi
1	T1	0	-190	-340	-530	-730	-990
	T2	0	-100	-160	-240	-310	-420
	T3	0	40	60	120	160	210
3	T4	0	-160	-270	-360	-420	-470
	T5	0	-240	-390	-550	-740	-970
	T6	0	-260	-420	-570	-670	-770
5	T7	0	-250	-420	-540	-610	-660
	T8	0	-280	-450	-560	-620	-670
	T9	0	-280	-430	-550	-620	-660
		Bottom Face					
2	B1	0	260	310	340	320	280
	B2	0	130	160	180	190	190
	B3	0	-60	-70	-50	-20	20
4	B4	0	140	290	480	650	940
	B5	0	250	420	620	740	890
	B6	0	230	380	560	690	820
6	B7	0	220	450	690	870	1050
	B8	0	250	460	700	880	1040
	B9	0	260	480	630	850	1010



TABLE VII

## ROSETTE STRAIN GAGES

PRINCIPAL STRAINS & STRESSES  
ANGLE TO PRINCIPAL STRESS

## Top Face

## #1 Rosette (45°)

Load psi	$\epsilon_{min}$	$\epsilon_{max}$	$\sigma_{min}$ psi	$\sigma_{max}$ psi	Angle to $\sigma_{min}$
0.00	0	0	0	0	0
0.25	-192.7	42.7	-2006	-242	6.13° cw
0.50	-340.5	60.5	-3608	-596	2.85 cw
0.75	-531.8	126.8	-5530	-586	3.07 cw
1.00	-730.7	160.7	-7620	-933	1.61 cw
1.25	-990.7	210.7	-10,360	-1344	1.43 cw

## #3 Rosette (120°)

0.00	0	0	0	0	0
0.25	-281.1	-158.9	-3740	-2823	5.45° cw
0.50	-511.0	-209.0	-6510	-4230	3.29 cw
0.75	-703.7	-282.9	-8940	-5770	1.57 cw
1.00	-927.2	-326.2	-10,480	-6720	1.98 cw
1.25	-1060.6	-359.4	-12,110	-7590	1.65 cw

## #5 Rosette (45°)

0.00	0	0	0	0	0
0.25	-284.1	-255.9	-4155	-3950	22.50° cw
0.50	-450.5	-399.5	-6560	-6190	39.34 cw
0.75	-560.8	-529.2	-8294	-8060	35.78 cw
1.00	-622.1	-607.9	-9270	-9180	22.50 cw
1.25	-670.0	-650.0	-9980	-9830	45.00 cw

(1) Angle is measured clockwise, cw, or counterclockwise, ccw, from the right side of a tangential axis passed through center of rosette.





TABLE IX

## ROSETTE STRAIN GAUGES

PRINCIPAL STRAINS & STRESSES  
ANGLE TO PRINCIPAL STRESS

Bottom Face

# 2 Rosette ( $45^\circ$ )

Load psi	$\epsilon_{\min}$	$\epsilon_{\max}$	$\sigma_{\min}$ psi	$\sigma_{\max}$ psi	Angle to $\sigma_{\max(1)}$
0.00	0	0	0	0	0
0.25	-62.8	262.8	279	2722	$5.31^\circ$ cw
0.50	-74.2	314.2	344	3255	$5.2^\circ$ cw
0.75	-54.1	343.8	682	3600	$5.09^\circ$ cw
1.00	-24.6	324.6	941	3560	$6.62^\circ$ cw
1.25	14.0	280.0	1230	3270	$8.5^\circ$ cw

# 4 Rosette ( $120^\circ$ )

0.00	0	0	0	0	0
0.25	139.0	274.3	2575	3593	$4.95^\circ$ cw
0.50	288.4	440.3	4840	6000	$8.30^\circ$ cw
0.75	472.2	634.4	7650	8860	$12.60^\circ$ cw
1.00	637.1	742.9	9900	10690	$20.45^\circ$ cw
1.25	811.3	882.0	12380	12900	$20.46^\circ$ cw

# 6 Rosette ( $45^\circ$ )

0.00	0	0	0	0	0
0.25	217.6	262.4	3433	3767	$13.29^\circ$ ccw
0.50	442.2	480.8	6850	7095	$9.21^\circ$ cw
0.75	669.2	700.8	10160	10390	$54.22^\circ$ ccw
1.00	837.6	882.4	12730	13070	$58.29^\circ$ ccw
1.25	1067.6	1052.4	15270	15620	$76.71^\circ$ ccw

$$E = 10^7 \text{ psi} \quad \mu = 1/3$$

(1) Angle is measured clockwise, cw, or counterclockwise, ccw, from the right side of a tangential axis passed through the center of the rosette.



TABLE X

## GAGE FACTOR

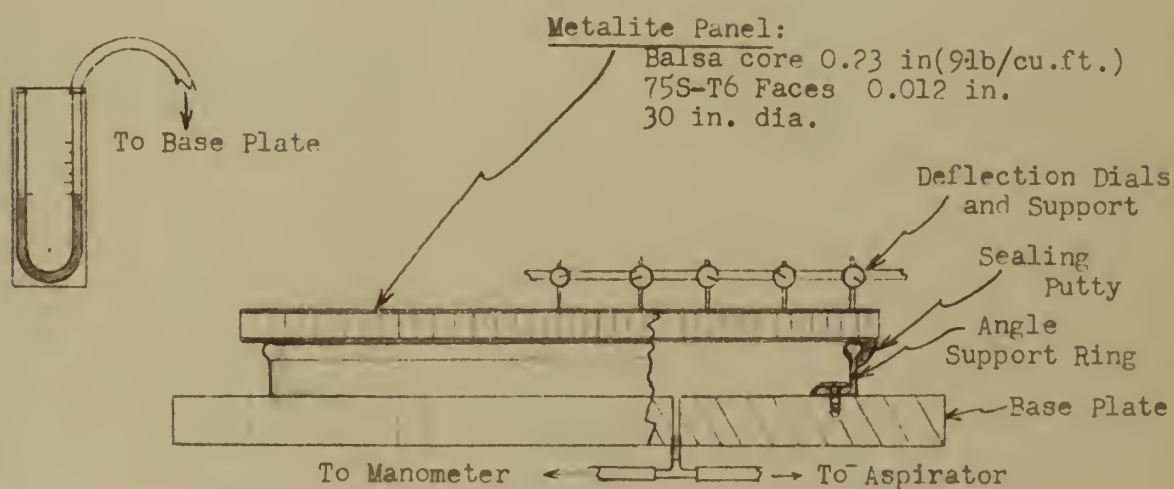
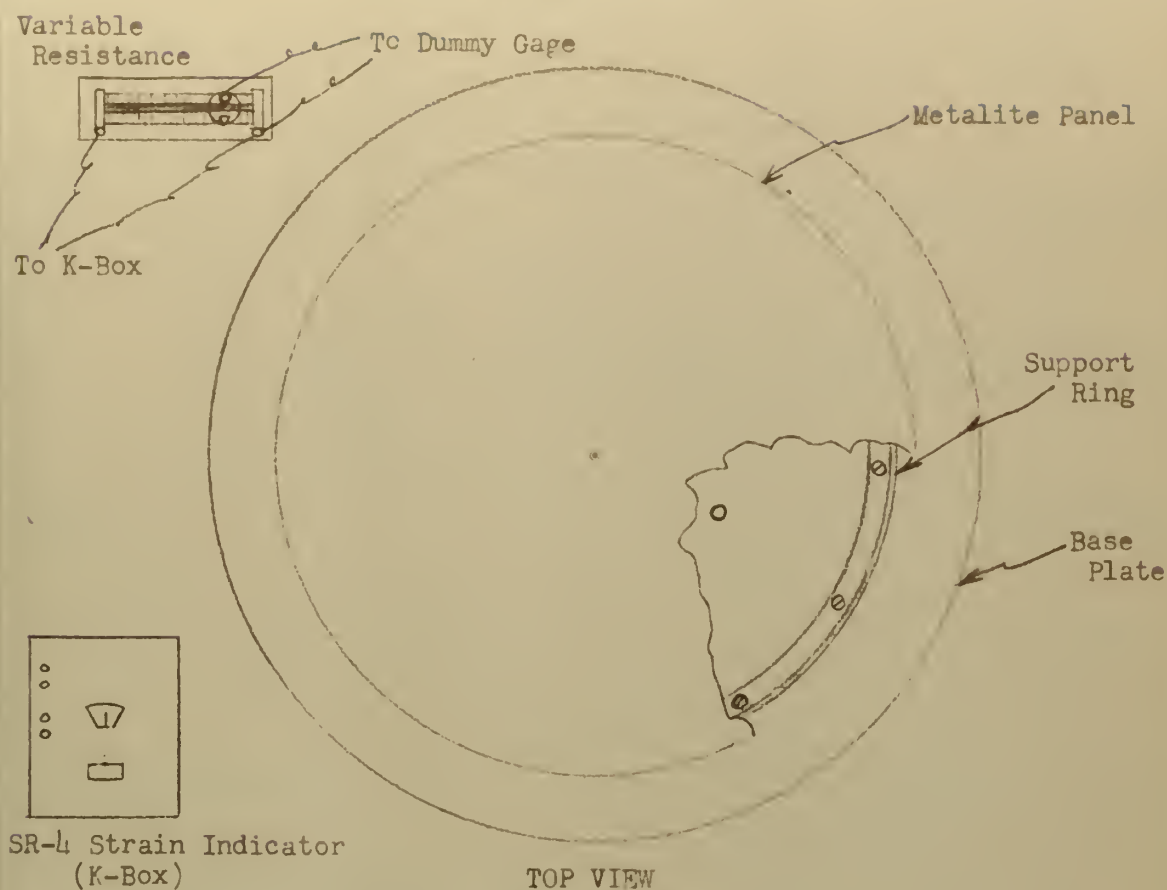
## TENSION LOAD vs STRAIN

Load psi	Gage Factor 1.77	Gage Factor 2.04	Gage Factor 2.20
	Micro inches	Micro inches	Micro inches
0	0	0	0
2000	180	140	140
4000	350	300	280
6000	525	450	420
8000	715	610	560
10000	880	780	710



Fig. 1

## TESTING EQUIPMENT



SIDE VIEW

(Not to scale)





Fig. 2

## SINGLE WIRE STRAIN GAGES

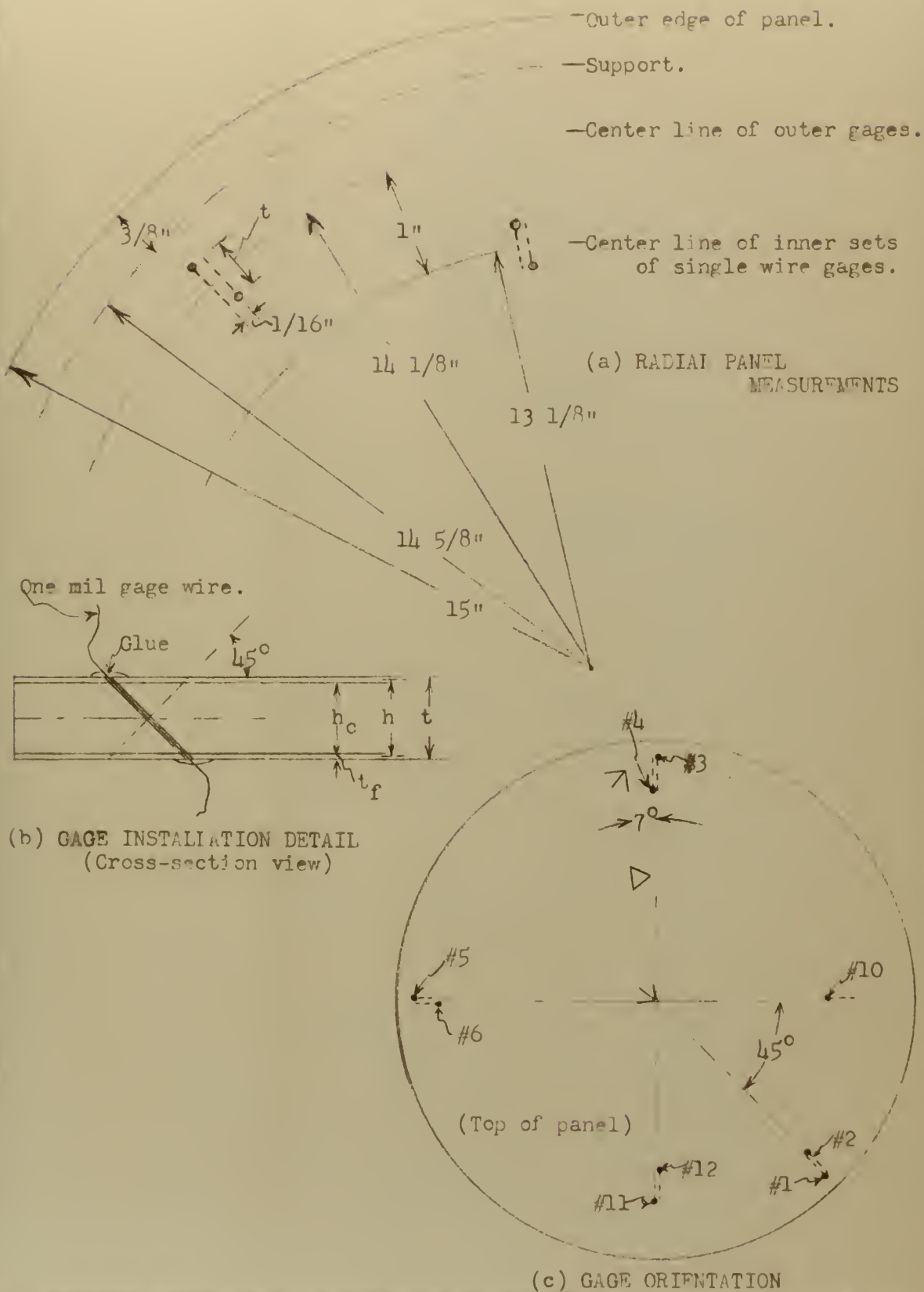
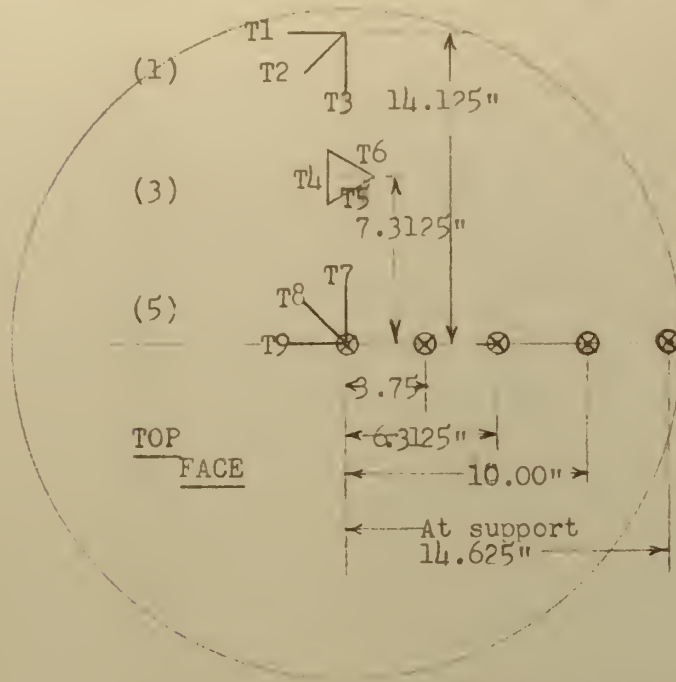




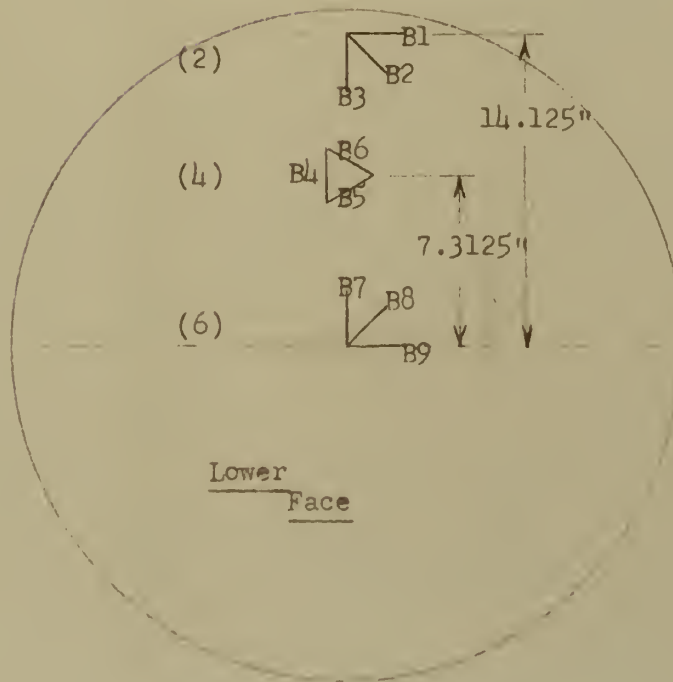
Fig. 3

## POSITIONING OF ROSETTE &amp; AMES GAGES



( ) Rosette Numbers

⊗ Ames Dial Deflection Gages







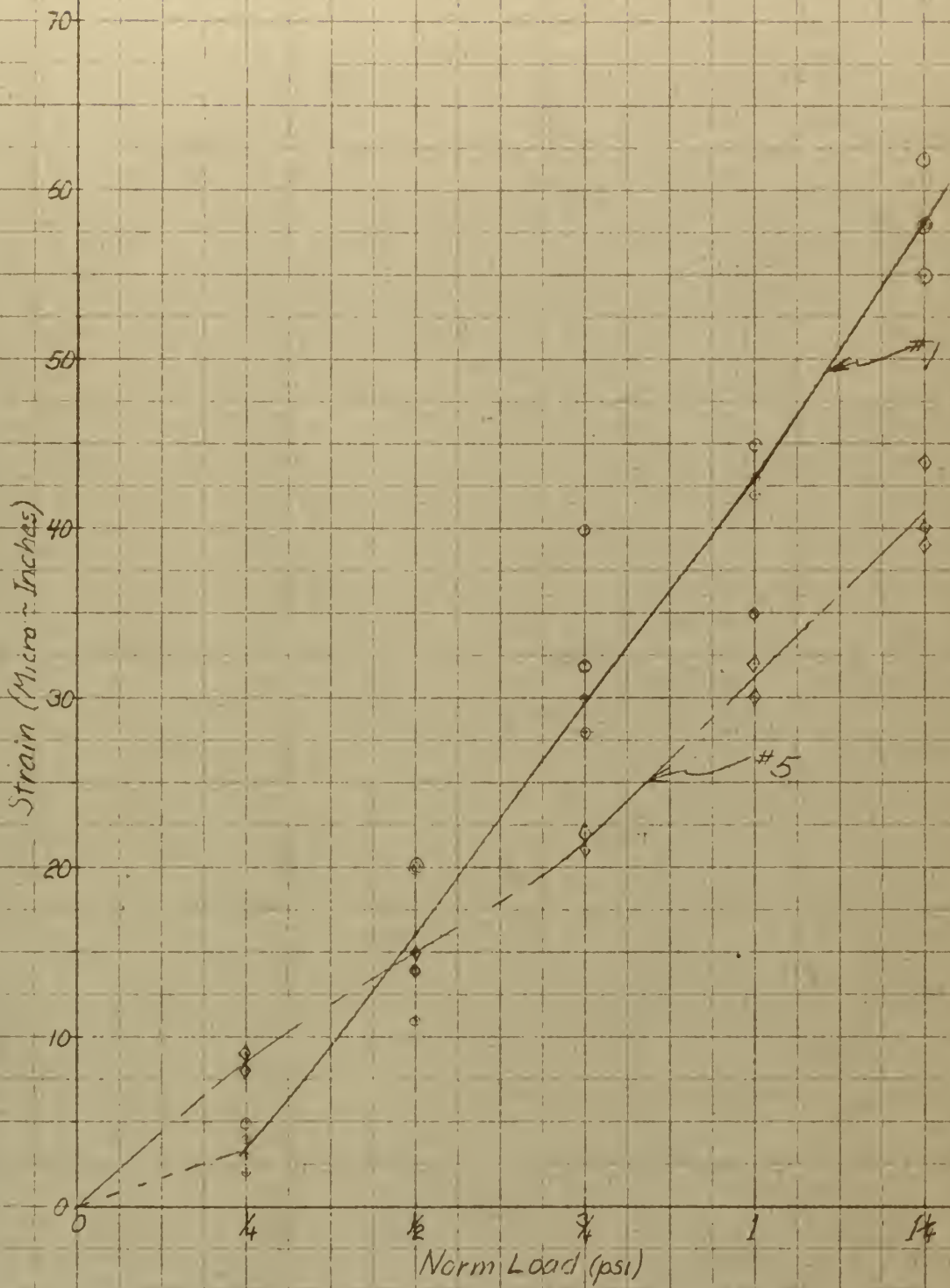


Fig. 4  
Strain-Loading Curve  
Gages #1 & #5  
(G.F. not corrected)



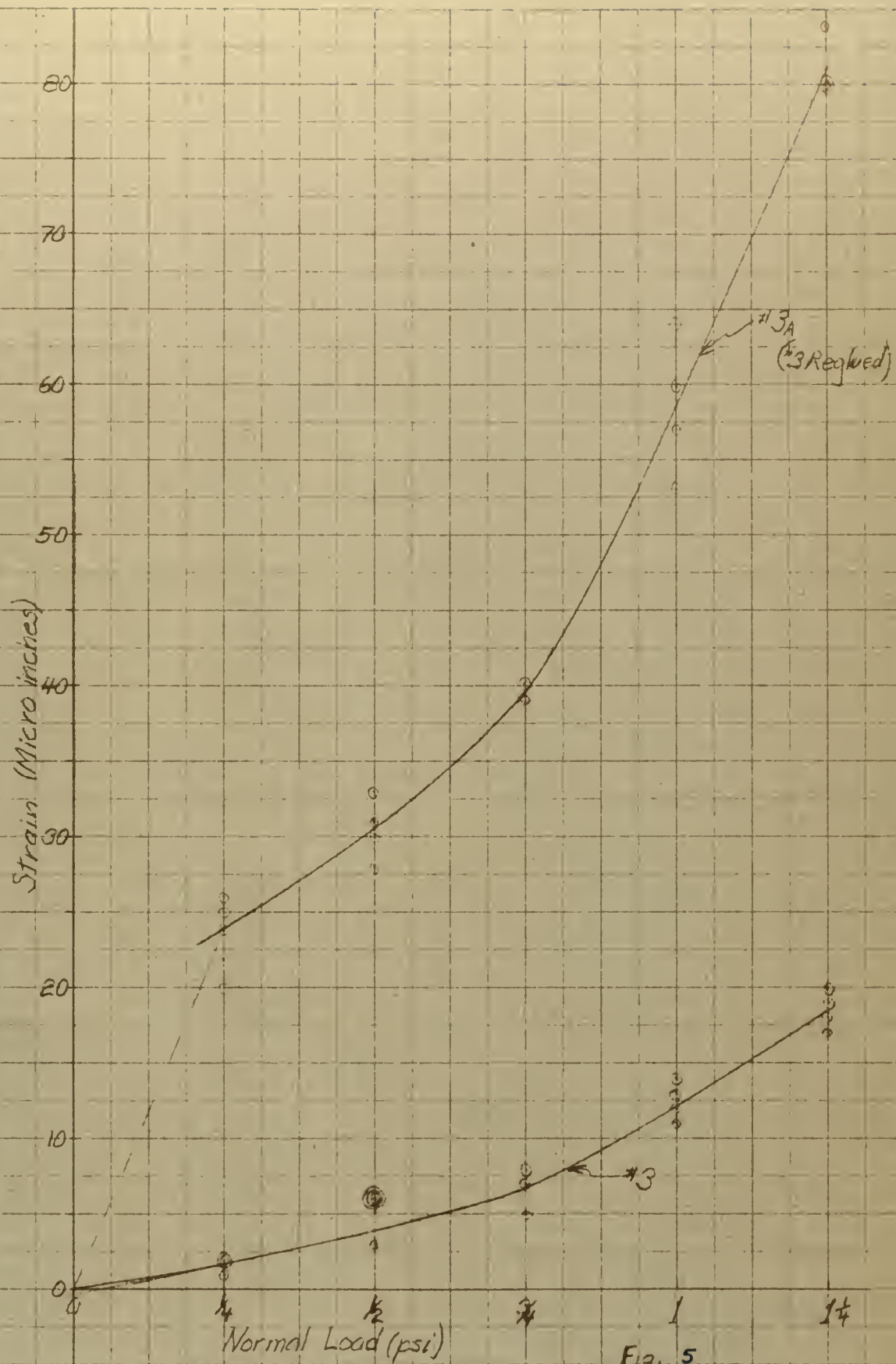


Fig. 5  
Strain ~ Loading Curves  
Gages #3 & #3A  
(Uncorrected for G.F.)





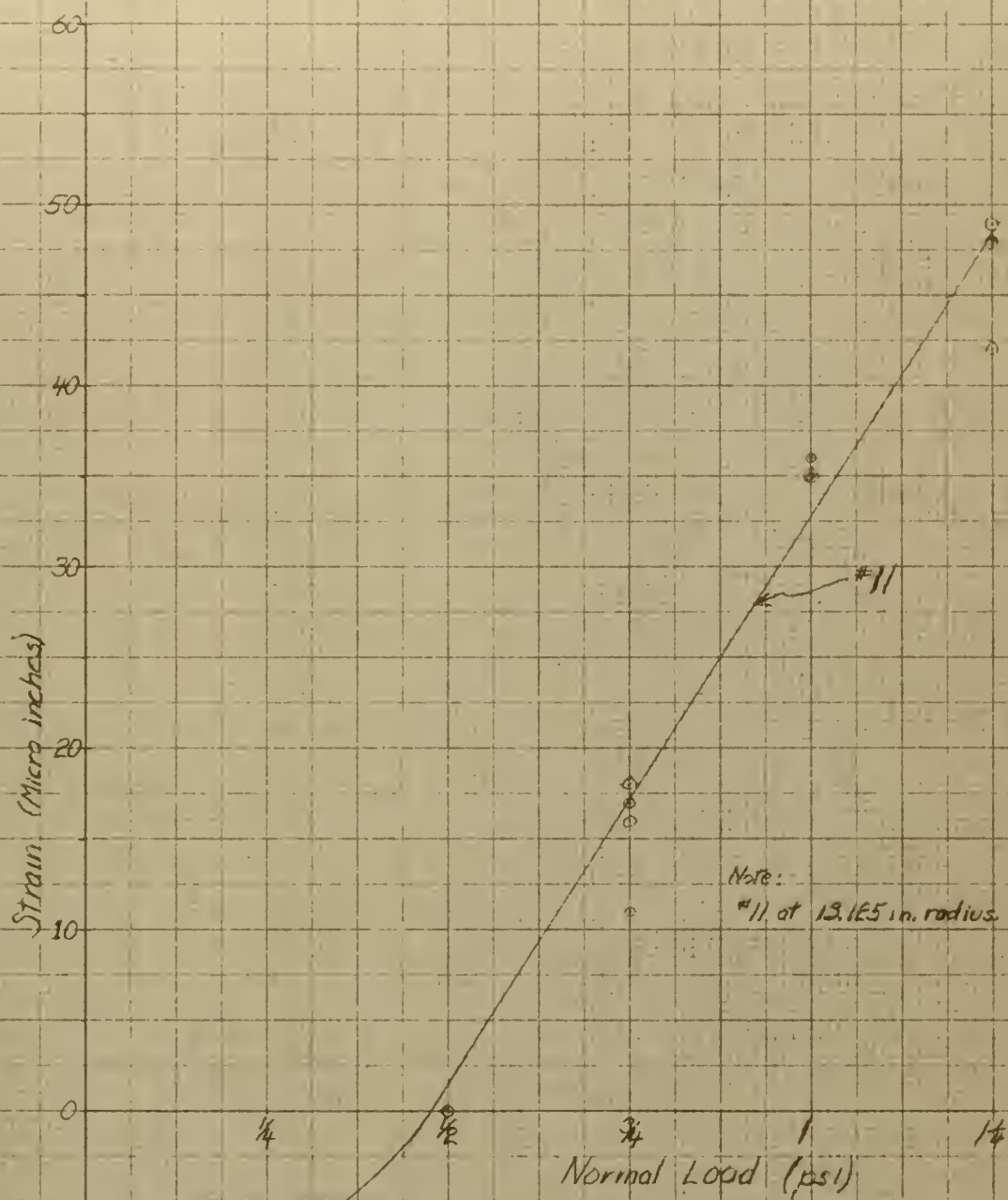


Fig. 6  
Strain ~ Loading Curve  
Gage #11  
(Not corrected for G.F.)





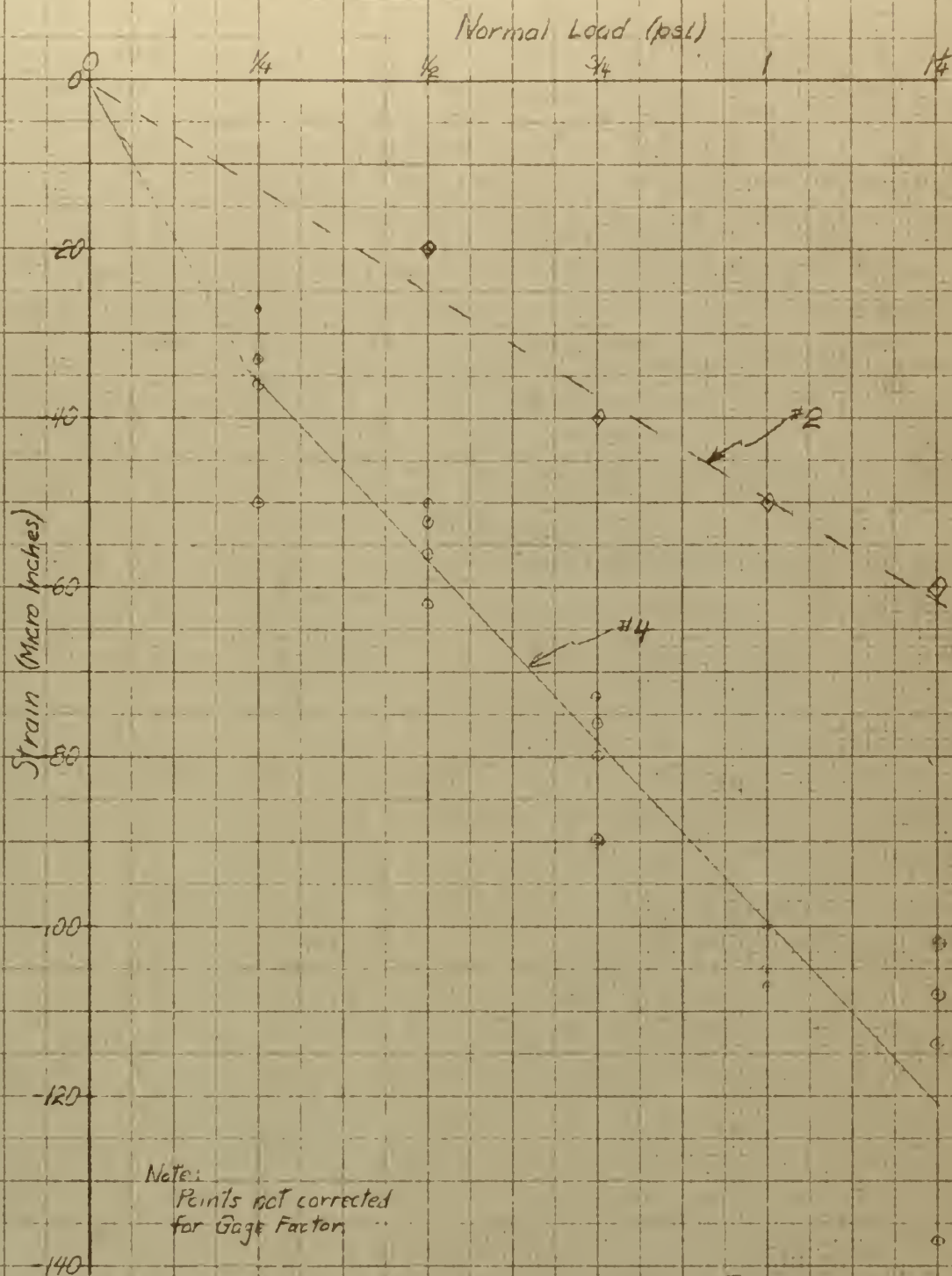


Fig. 7  
Strain ~ Loading Curves  
Gages #2 & #4  
(at 14.125 in radius)  
CHG



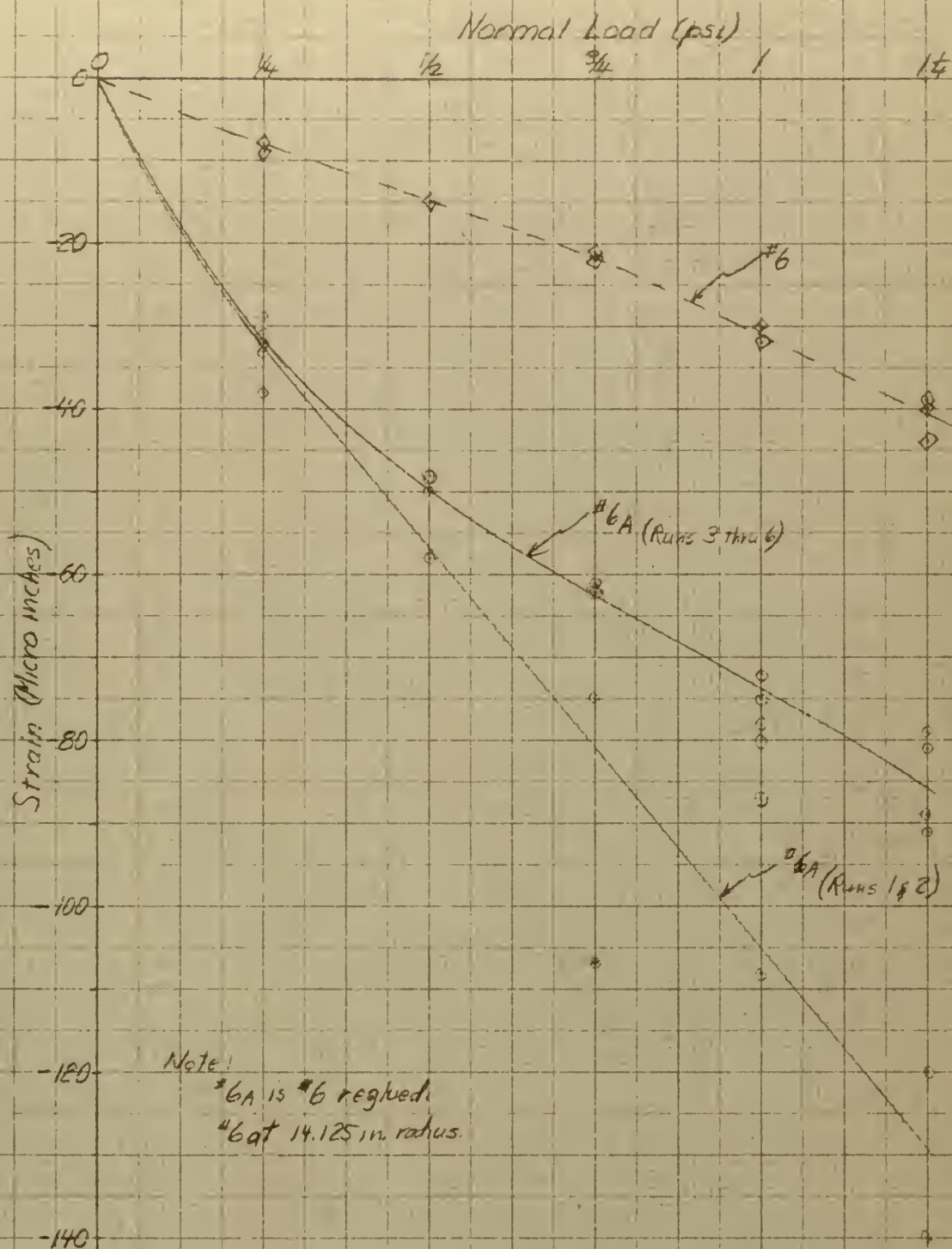


Fig. 8  
 Strain ~ Loading Curves  
 Gage #6  
 (Not corrected for G.F.)

CHG





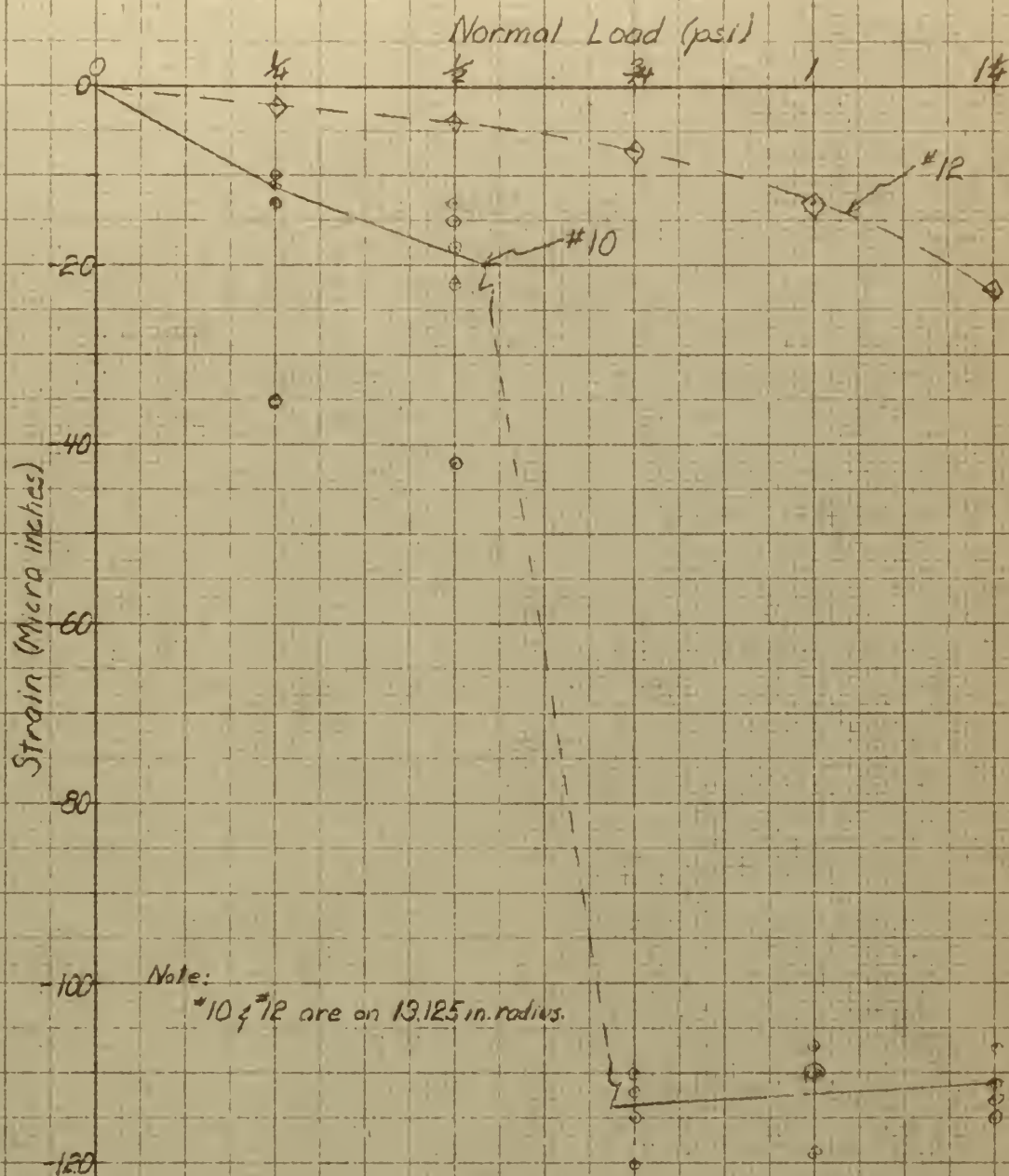
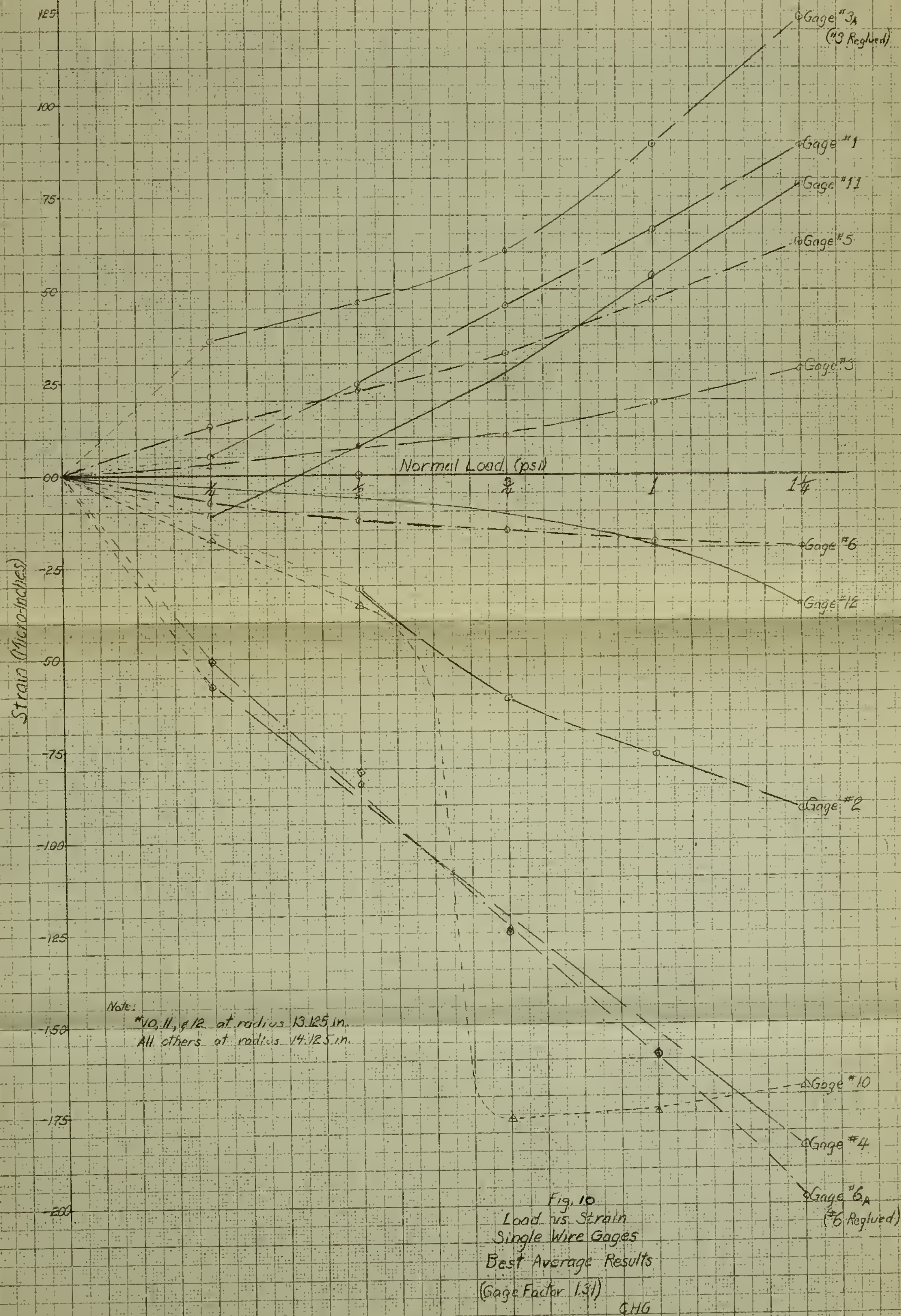


Fig. 9  
Strain - Loading Curve  
Gages #10 & #12  
(Not corrected for G.F.)











Note:

Rosettes #1 & #6 opposing faces of 14.125 in. radius.

" #3 & #4 " " " 7.3125 " "

" #5 & #6 " " " panel center

Rosettes #1, #3, & #5 on top face.

" #2, #4, & #6 " lower " "

$\sigma$  - Stress (psi)  
(Tension (+)  
Compression (-))

$\pm 16,000$   
 $\pm 14,000$   
 $\pm 12,000$   
 $\pm 10,000$   
 $\pm 8,000$   
 $\pm 6,000$   
 $\pm 4,000$   
 $\pm 2,000$

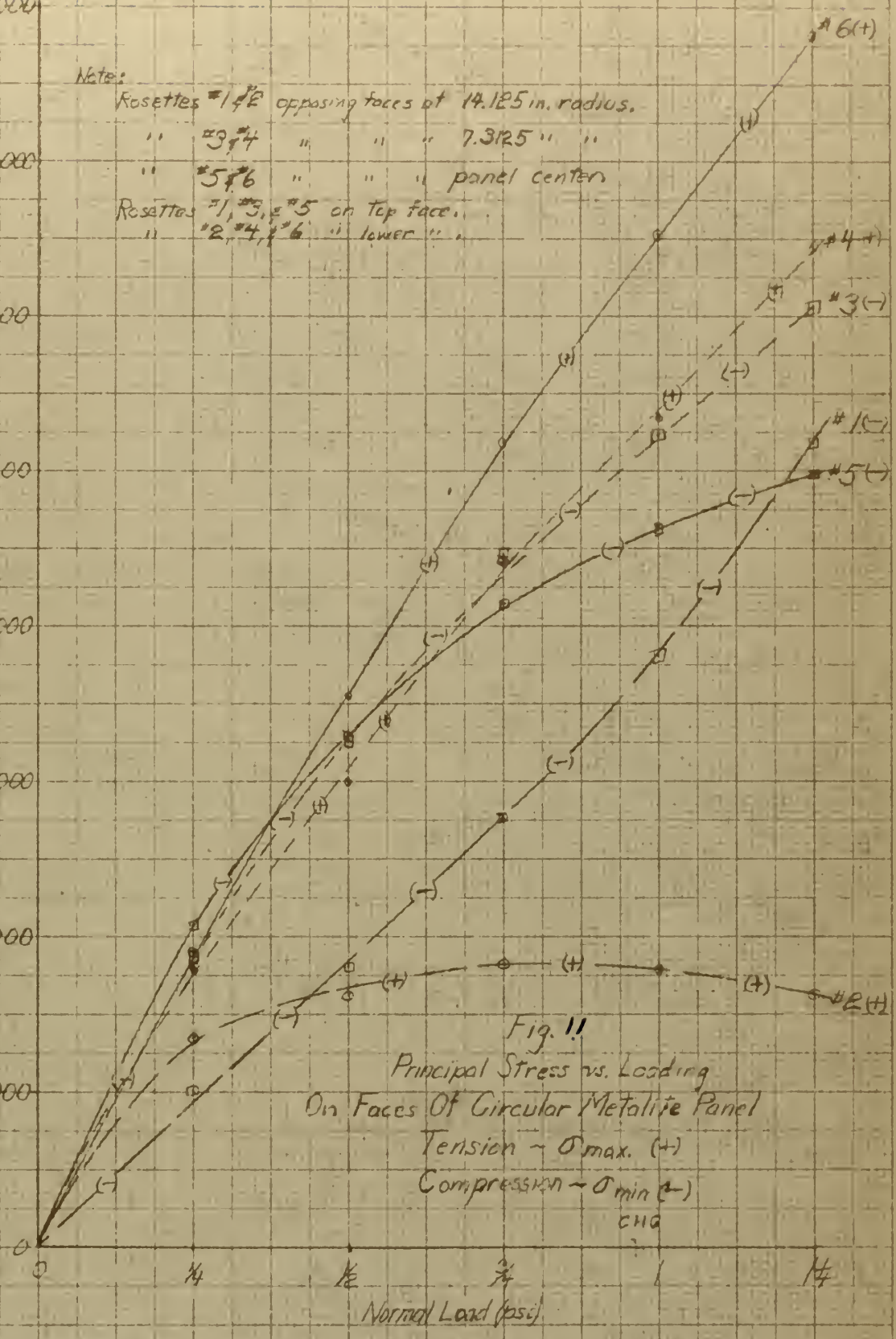


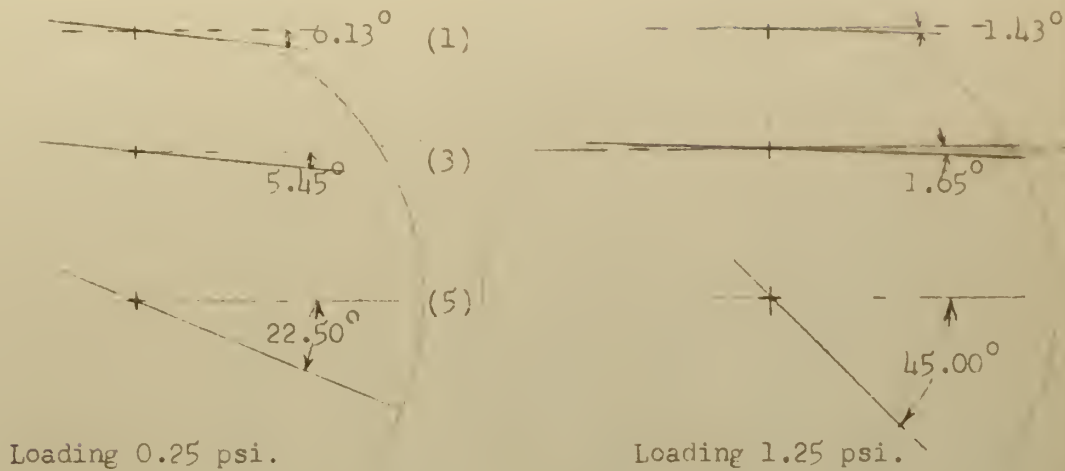
Fig. 11  
Principal Stress vs. Loading  
On Faces Of Circular Metalite Panel  
Tension -  $\sigma_{max}$  (+)  
Compression -  $\sigma_{min}$  (-)  
CHD

Normal Load (psi)

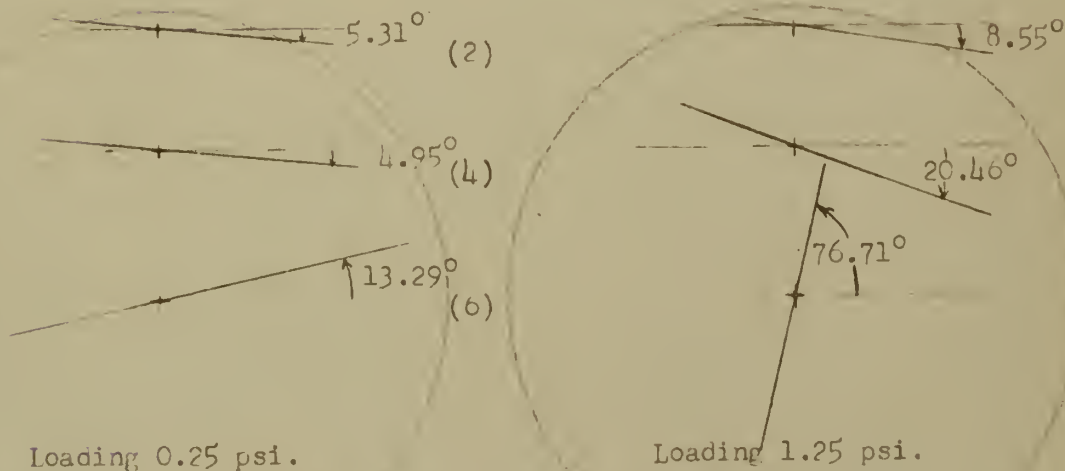




Fig. 12  
ANGLES TO PRINCIPAL AXIS  
 (Rosette Gages)



TOP FACE  
 ( $\sigma_{\min}$  - Compression)



LOWER FACE  
 ( $\sigma_{\max}$  - Tension)

( ) Rosette Numbers



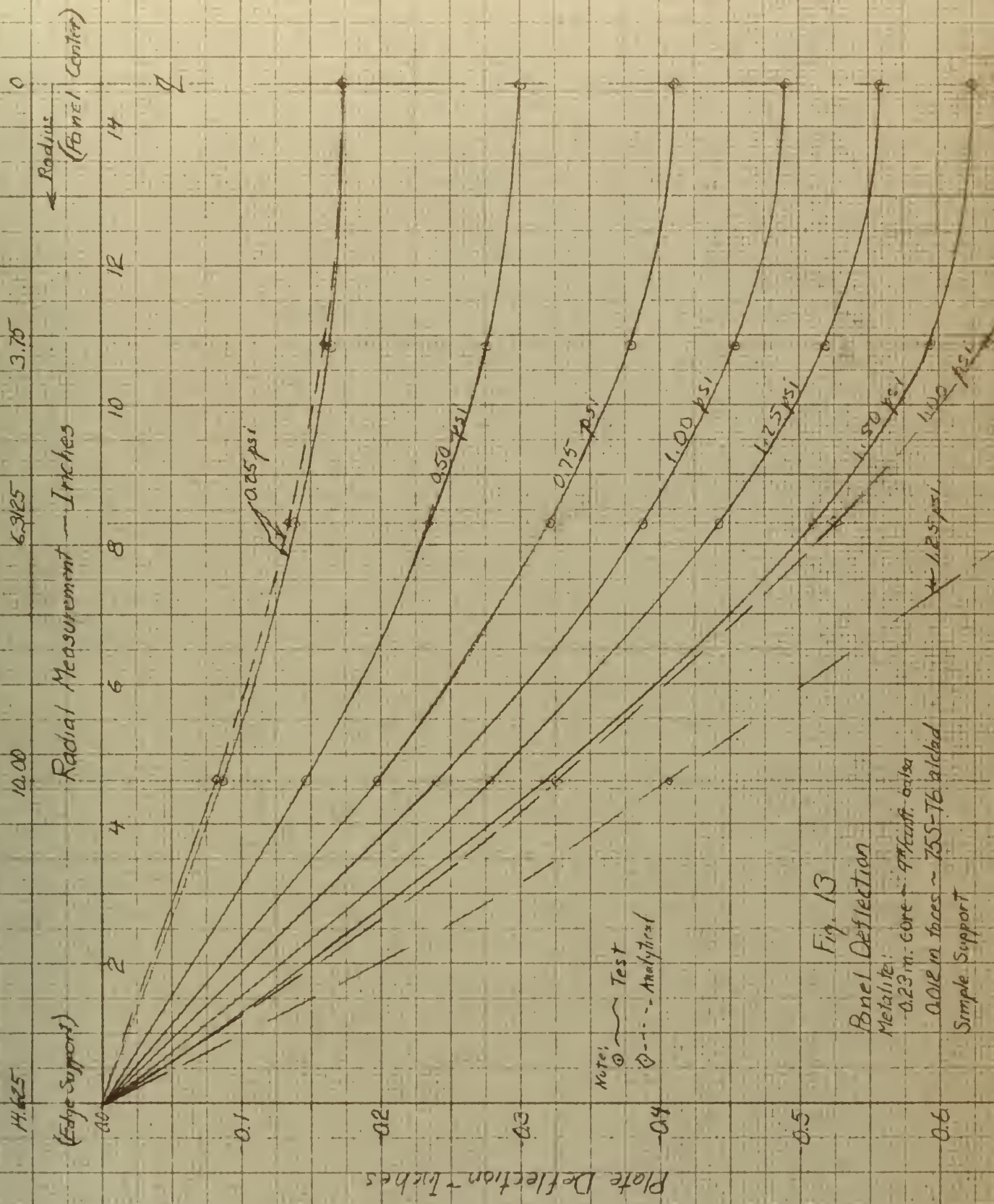


Fig. 13

Panel Deflection

Material:

0.23 in. core - 97% cast.alsa

0.012 in. faces - 75S-T6 alclad

Simple Support





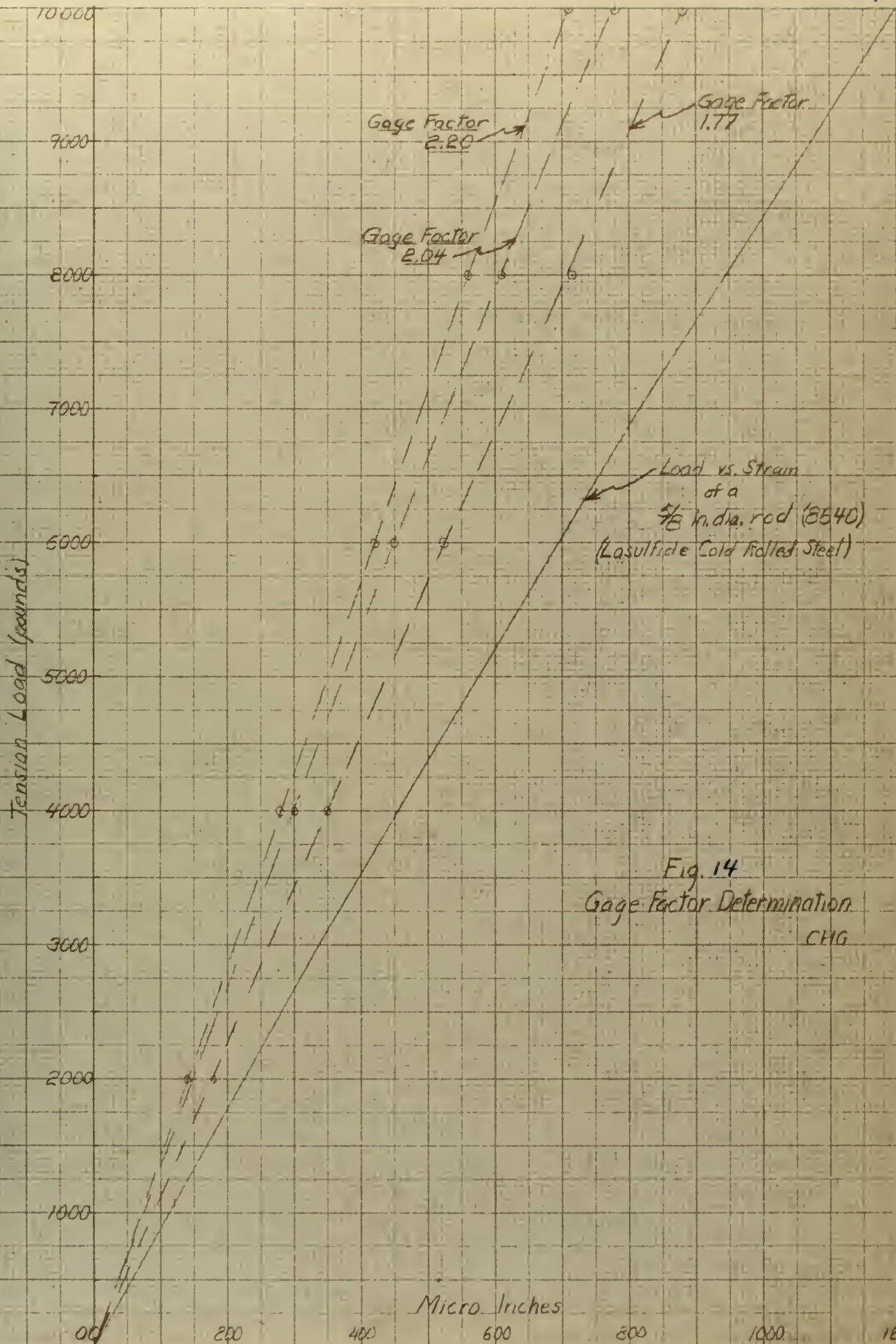


Fig. 14  
Gage Factor Determination  
CHG







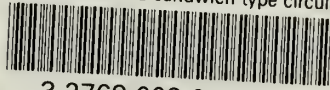


pla



thesG25

Investigation of a sandwich type circula



3 2768 002 01092 8

DUDLEY KNOX LIBRARY